PENSOFT
SENCKENBERG world of biodiversity
Leibniz Association

The development of nasal turbinal morphology of moles and shrews

Festschrift in Honour of Professor Dr. Wolfgang Maier
Edited by Ingmar Werneburg & Irina Ruf

Kai Ito[1,2], Ryo Kodeara[2], Kazuhiko Koyasu[3], Quentin Martinez[4], Daisuke Koyabu[5]

1 *Department of Natural Environmental Studies, Graduate School of Frontier Sciences, The University of Tokyo, 5-1-5 Kashiwanoha, Kashiwa-shi, Chiba 277-0882, Japan*
2 *Department of Anatomy, School of Dental Medicine, Tsurumi University, 2-1-3 Tsurumi, Tsurumi-ku, Yokohama 230-8501, Japan*
3 *Department of Anatomy, School of Dentitstry, Aichi Gakuin University, 1-100 Kusumoto, Nagoya 464-8650, Japan*
4 *State Museum of Natural History, Rosenstein 1, 70191 Stuttgart, Germany*
5 *Research and Development Center for Precision Medicine, University of Tsukuba, 1-2 Kasuga, Tsukuba-shi, Ibaraki 305-8550 Japan*

http://zoobank.org/References/65A25994-19FF-4034-BA2C-6A2D2530C493

Corresponding author: Kai Ito (ocean42.rhino@gmail.com)

Academic editor Irina Ruf | **Received** 18 April 2022 | **Accepted** 15 July 2022 | **Published** 28 September 2022

Citation: Ito K, Kodeara R, Koyasu K, Martinez Q, Koyabu D (2022) The development of nasal turbinal morphology of moles and shrews. Vertebrate Zoology 72 857–881. https://doi.org/10.3897/vz.72.e85466

Abstract

The phylogenetic relationships of major groups within the Order Eulipotyphla was once highly disputed, but the advent of molecular studies has greatly improved our understanding about the diversification history of talpids, soricids, erinaceids, and solenodontids. Their resolved phylogenetic relationships now allow us to revisit the turbinal and lamina evolution of this group. The inner structure of the nasal cavity of mammals is highly complicated and the homologies of the turbinals among mammalian species are still largely unsettled. In this regard, investigation on fetal anatomy and ontogenetic changes of the nasal capsule allows us to evaluate the homologies of the turbinals and laminae. We observed various fetuses and adults of talpids and soricids using high-resolution diffusible iodine-based contrast-enhanced computed tomography (diceCT) and reviewed previous reports on erinaceids, solenodontids, and other laurasiatherians. Although the turbinal and lamina morphology was previsouly considered to be similar among eulipotyphlans, we found phylogenetic patterns for talpids and soricids. The nasoturbinal of the common ancestor of talpids and soricids was most likely rostrocaudally elongated. The epiturbinal at the ethmoturbinal II disappeared in soricids independently. Finally, we propose two possible scenarios for the maxilloturbinal development: 1) the maxilloturbinal of talpids and soricids became small independently with a limited number of lamellae as a result of convergent evolution, or 2) the common ancestor of talpids and soricids already had a small and simple maxilloturbinal.

Keywords

eulipotyphlans, evo-devo, homology, microCT (μCT), skull

Introduction

Mammals have plate-like structures called turbinals in the nasal cavity which possess bony or cartilaginous plate-like structures inside them (Moore 1981; Smith et al. 2015; Smith et al. 2021a). The turbinal expands the surface area in the nasal cavity by complex branching and scrolling (Parker 1874; Parker 1885; Martineau-Doizé et al. 1992; Smith et al. 2021a, 2021b). Depending on their localization, the tissue on the surface of the turbinal is characterized by a large number of secretory goblet cells and capillaries and olfactory receptors (Negus 1958; Smith et al. 2021b). Therefore, the turbinals have functions, such as warming the air from the outside world and absorbing water from the exhaled breath, and a role in olfaction (Negus 1958; Hillenius 1992).

The terminology for turbinals differs among researchers which have often hindered the progress of turbinal research (Rowe et al. 2005; Maier and Ruf 2014; Ruf 2014) (Table 1). Paulli established the first set of terminology (Paulli 1900a, 1900b, 1900c). The larger main turbinals are the endoturbinals, and the turbinals between the endoturbinals are the ectoturbinals. Each turbinal is numbered from the dorsal side. Nonetheless, this terminology is not suited to address homology problems of the turbinal because it does not take topography and ontogeny into account (Maier and Ruf 2014; Ruf 2014). For example, considering ontogeny, the structure that is lamina instead of turbinal is represented as endoturbinal 1, and all small-shaped turbinals are represented as ectoturbinals together. On the other hand, the terminology used by Voit (1909) and others (Reinbach 1952a, 1952b; Maier 1993a, 1993b) is based on ontogeny, which is well-suited to examine the homology between distant species. Therefore, we followed the anatomical terminology of Voit (1909) and the bauplan advocated by Maier (1993a) (Fig. 1).

Types of the turbinal include the marginoturbinal, atrioturbinal, nasoturbinal, maxilloturbinal, ethmoturbinal, epiturbinal, frontoturbinal, and interturbinal (Maier 1993a, 1993b). The marginoturbinal continues into the atrioturbinal and forms the frame external naris (Maier 1980, 2000; Göbbel 2000). These turbinals which form the rostral part of the nasal cavity do not ossify (Zeller 1987; Maier 2014, 2020; Smith et al. 2015). In addition, the marginoturbinal and the atrioturbinal are attached to facial muscles. As a result, this structure changes the shape of the naris and controls the inflow and outflow of air (Göbbel 2000; Maier and Ruf 2014). These turbinals are covered with a keratinous epithelium (Ruf 2020).

The nasoturbinal is a rostrocaudally elongated structure that extends from near the naris to the dorsal side of the nasal cavity (Moore 1981). The maxilloturbinal is located on the rostroventral side of the nasal cavity and has a complex branched structure in some mammals (Negus 1958; Van Valkenburgh et al. 2004, 2014b; Maier and Ruf 2014; Smith et al. 2015). The nasoturbinal and maxilloturbinal are covered with a respiratory epithelium, which serves to moisten and warm the inhaled air (Negus 1958; Smith and Rossie 2008; Van Valkenburgh et al. 2014b; Martinez et al. 2018; Wagner and Ruf 2019).

Several ethmoturbinals are on the caudal side of the nasal cavity and are fused to the ethmoid bone (Van Gilse 1927; Smith et al. 2015). Under Voit's framework, Roman numerals are assigned from the rostral side to the caudal side to refer to the ethmoturbinals (Voit 1909). Among them, ethmoturbinal I is the largest and branches into the rostral and caudal sides (Voit 1909; Maier 1993a; Ruf 2020). Some studies name the caudal side of the branch as the ethmoturbinal II (Smith et al. 2007; Smith and Rossie 2008; Wible 2008). From each ethmoturbinal extend several small lamellae that serve as accessories (Maier 1993b). The turbinal formed from this branch is called the epiturbinal, which is unusual as turbinals commonly protrude from the inner wall of the nasal cavity (Maier 1993b; Smith and Rossie 2008).

There are multiple frontoturbinals in the frontoturbinal recess, which is the dorsal space of the lateral recess of the nasal cavity (Maier 1993a, 1993b; Rossie 2006). Multiple interturbinals are found in the frontoturbinal recess and the ethmoturbinal recess, which is the caudal recess of the nasal cavity. The interturbinals project from the inner wall of the nasal cavity, but do not project as far medially as other turbinals (Maier 1993a, 1993b). The ethmoturbinal, epiturbinal, frontoturbinal, and interturbinal are covered with the olfactory epithelium containing olfactory receptors (Le Gros Clark 1951; Van Valkenburgh et al. 2014a). The number of these turbinals varies widely between species (Paulli 1900a, 1900b, 1900c).

In addition to turbinals, three laminae are found in the nasal cavity. The lamina semicircularis projects behind the nasoturbinal (Maier 1993a, 1993b). The lamina horizontalis (also known as frontomaxillary septum) divides the lateral recess of the nasal cavity into two parts: dorsal and ventral (Rossie 2006; Smith and Rossie 2008; Maier and Ruf 2014). The dorsal side is the frontoturbinal recess and the ventral side is the maxillary recess (Ruf 2014). The lamina transversalis is a continuous structure that extends from the lateral wall to the nasal septum, dividing the ethmoturbinal recess and the nasopharyngeal duct (Lozanoff and Diewert 1989). The lamina transversalis continues from the lamina horizontalis and extends from the lateral wall to the nasal septum (Lozanoff and Diewert 1989; Macrini 2012; Smith et al. 2015).

The nasal capsule develops at the rostral part of the chondrocranium (Moore 1981; Kaucka et al. 2018). The basic structure of the turbinal and the lamina project into the nasal capsule (Dieulafe 1906; Ruf 2020). Some cartilages of the turbinal and the lamina are formed when the nasal capsule is formed, and some protrude from the inner wall of the nasal capsule after the formation of the nasal capsule (de Beer 1937; Smith and Rossie 2008; Van Valkenburgh et al. 2014b).

Morphogenesis of the nasal capsule in mammals is completed through three mesenchymal condensations: the parietotectal cartilage aside from the tectum (pars anterior), the paranasal cartilage (pars lateralis), and the orbitonasal lamina (pars posterior; de Beer 1937; Reinbach 1952b; Moore 1981; Zeller 1987; Rossie 2006;

Table 1. Terminology for turbinals and laminas of eulipotyphlans.

Structure name	Synonyms from other authors
Marginoturbinal	—
Atrioturbinal	—
Maxilloturbinal	Inferior concha (Moore 1981, p 255), inferior turbinal (Parker 1885)
Nasoturbinal	Nasal turbinal (Parker 1885), crus orale of the nasoturbinal (Woehrmann-Repenning and Meinel 1977)
Lamina semicircularis	Nasal turbinal (Parker 1885), endoturbinal I (Paulli 1900c; Sharma 1958; Schmidt and Nadolski 1979; Kuramoto 1980; Moore 1981), crista semicircularis (Voit 1909; Fawcett 1918; Michelsson 1922; de Beer 1929; Roux 1947; Youssef 1971), internal olfactory concha I and constriction (Ganeshina et al. 1957), olfactory turbinal 1 (Gurtovoi 1966), constriction crus intermedium of the nasoturbinal (Woehrmann-Repenning and Meinel 1977), nasoturbinal (Söllner and Kraft 1980; Larochelle and Baron 1989), nasoturbinal, ethmoid (Wible 2008)
Lamina horizontalis	Middle turbinal (Parker 1885), horizontally positioned lamella (Michelsson 1922), anterior root of ethmoturbinal I (de Beer 1929, 1937; Youssef 1971), crus intermedium and crus aborale of the nasoturbinal (Woehrmann-Repenning and Meinel 1977), a part of endoturbinal I (Larochelle and Baron 1989)
Ethmoturbinal I anterior part	Endoturbinal I (Allen 1882; Söllner and Kraft 1980; Larochelle and Baron 1989), middle turbinal (Parker 1885), endoturbinal II (Paulli 1900c; Moore 1981), ethmoturbinal 1 (de Beer 1929; Ioana 1970), dorsal lamella of first primary (Roux 1947), internal turbinal II[1] (Ganeshina et al. 1957), endoturbinal II a (Sharma 1958), upper roll of olfactory turbinal 4 (Gurtovoi 1966), dorsal lamella of first primary ethinoturbinal (Youssef 1971), endoturbinal II' (Schmidt and Nadolski 1979; Kuramoto 1980), middle concha (Moore 1981 p255)
Ethmoturbinal I posterior part	Ethmoturbinal I lobule (Allen 1882), middle turbinal (Parker 1885), Endoturbinal II lower lamella (Paulli 1990 c; Moore 1981), accessory lamina at ethmoturbinal I (Michelsson 1922), ethmoturbinal 1 (de Beer 1929; Ioana 1970), ventral lamella of first primary ethmoturbinal (Roux 1947), internal turbinal II[2] (Ganeshina et al. 1957), ethmoturbinal 2 (Ioana 1970), endoturbinal II b (Sharma 1958), lower roll of olfactory turbinal 4 (Gurtovoi 1966), ventral lamella of first primary ethinoturbinal (Youssef 1971), epiturbinal I (Woehrmann-Repenning and Meinel 1977), endoturbinal II'' (Schmidt and Nadolski 1979; Kuramoto 1980), epiturbinal at ethmoturbinal (Söllner and Kraft 1980), middle concha (Moore 1981, p 255), accessory lamellae of endoturbinal I (Larochelle and Baron 1989), ethmoturbinal II (Wible 2008)
Ethmoturbinal II	Endoturbinal II (Allen 1882; Söllner and Kraft 1980; Larochelle and Baron 1989), middle turbinal (Parker 1885), endoturbinal III (Paulli 1990c; Moore 1981; Sharma 1958; Schmidt and Nadolski 1979; Kuramoto 1980), superior concha (Moore 1981, p 255), internal turbinal III (Ganeshina et al. 1957), olfactory turbinal 6 (Gurtovoi 1966), ethmoturbinal 3 (Ioana 1970), superior concha (Moore 1981, p 255), ethmoturbinal III (Wible 2008)
Ethmoturbinal III	Endoturbinal III (Allen 1882; Söllner and Kraft 1980; Larochelle and Baron 1989), endoturbinal IV (Paulli 1990c; Moore 1981; Schmidt and Nadolski 1979; Kuramoto 1980), internal turbinal IV (Ganeshina et al. 1957), ectoturbinal III (Sharma 1958), olfactory turbinal 6 (Gurtovoi 1966), highest concha (Moore 1981 p255), ethmoturbinal 4 (Ioana 1970), ethmoturbinal IV (Wible 2008)
Frontoturbinal	Ectoturbinal (Allen 1882; Paulli 1900c; Sharma 1958; Woehrmann-Repenning and Meinel 1977; Schmidt and Nadolski 1979; Kuramoto 1980; Söllner and Kraft 1980; Moore 1981; Larochelle and Baron 1989; Wible 2008), upper turbinal (Parker 1885), concha frontalis (Michelsson 1922), secondary ethmoturbinal (Roux 1947), external olfactory turbinal (Ganeshina et al. 1957), olfactory turbinal 2 and 3 (Gurtovoi 1966)
Interturbinal	Ectoturbinal (Allen 1882; Paulli 1900c; Sharma 1958; Moore 1981; Larochelle and Baron 1989), ectoturbinal III (Woehrmann-Repenning and Meinel 1977; Schmidt and Nadolski 1979; Kuramoto 1980), secondary ethnoturbinal (Fawcett 1918; Roux 1947), olfactory turbinal 5 (Gurtovoi 1966)
Epiturbinal	External olfactory turbinal (Ganeshina et al. 1957), epiturbinal II (Woehrmann-Repenning and Meinel 1977)

Smith and Rossie 2006, 2008; Van Valkenburgh et al. 2014a). The paranasal cartilage covers the parietotectal cartilage and the orbitonasal lamina while each cartilage condenses (de Beer 1937; Smith and Rossie 2008; Van Valkenburgh et al. 2014a). On the rostral side, where the paranasal cartilage overlaps the parietotectal cartilage, the lamina semicircularis is formed from the parietotectal cartilage (Smith and Rossie 2008; Van Valkenburgh et al. 2014b). On the caudal side, where the the paranasal cartilage overlaps the orbitonasal lamina, the ethmoturbinal I is formed from the orbitonasal lamina (Smith and Rossie 2008; Van Valkenburgh et al. 2014a). The nasoturbinal, frontoturbinal, interturbinal, lamina horizontalis, and ethmoturbinals, other than ethmoturbinal I, project from the inner wall of the nasal capsule (Smith and Rossie 2008; Van Valkenburgh et al. 2014a). The ethmoturbinals II, III and IV project in this order from the area originating from the orbitonasal lamina (Rossie 2006; Smith and Rossie 2008; Van Valkenburgh et al. 2014a). The marginoturbinal, atrioturbinal, and maxilloturbinal are formed from the ventral margin of the nasal capsule.

Maier (1993b) showed that the nasal capsule structure, including the turbinal and lamina, does not vary among therian species, indicating the nasal capsule bauplans. From birth to adulthood, the turbinal and lamina become more complex, branching and scrolling as they grow (Maier and Ruf 2014). A part of the cartilage of the turbinal and the lamina become ossified, and a thin ossified plate is formed inside them (Smith et al. 2021a). This ossified plate binds to the maxilla and the ethmoid bone and merges with these bones. The nasal capsule is enclosed by exocranial facial bones (the palatine, maxilla, and nasal) and is integrated into the nasal cavity of the adult. As nasal capsules "become complex with growth", it is thus crucial to observe the structural changes of the nasal capsules during development and carefully track them by studying various developmental stages in order to examine the homology among distant species.

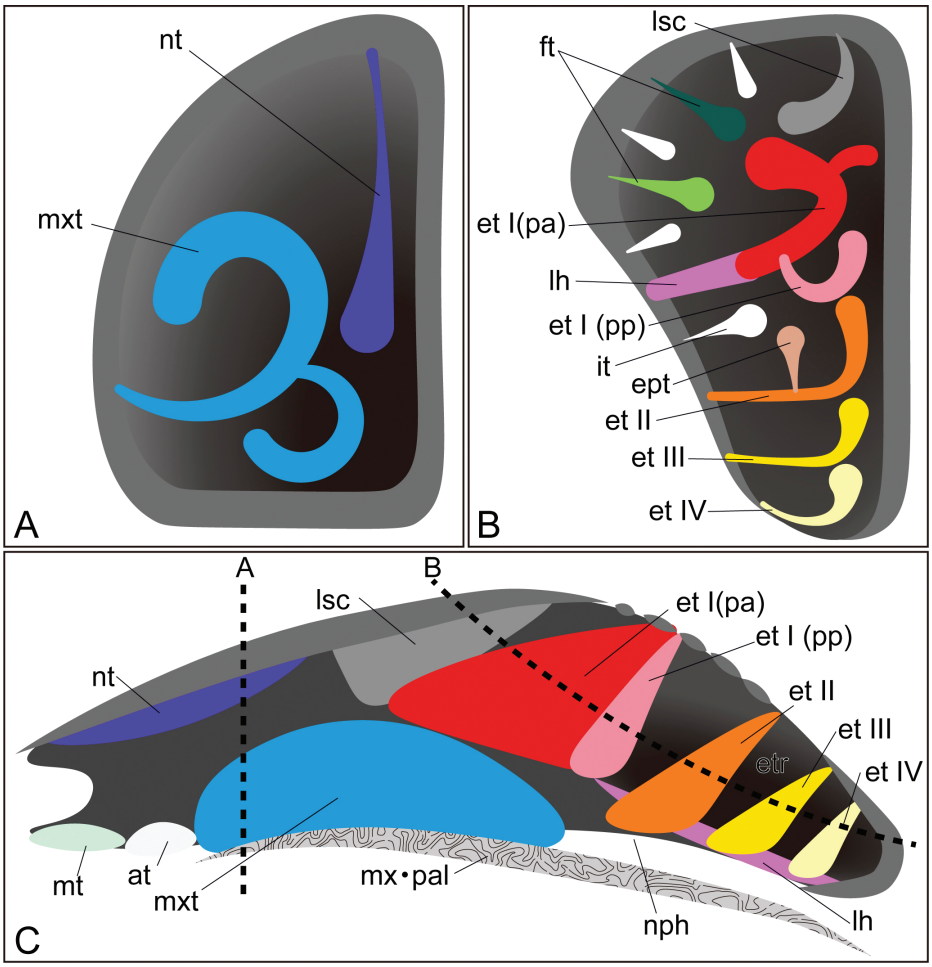

Figure 1. Generalised schematic mammalian nasal capsule. **A** Coronal section through the rostral part of the nasal capsule; **B** coronal section through the caudal part of the nasal capsule, modified from Maier (1993b); **C** medial view of parasagittal section modified from Maier (1993a) and Maier and Ruf (2014). These images show the nasal structure without facial exocranial (dermal) bones, except for the maxilla and palatine bones. Broken lines indicate each coronal section. Abbreviations: at = atrioturbinal; ept = epiturbinal; et I (pa) = ethmoturbinal I pars anterior; et I (pp) = ethmoturbinal I pars posterior; et II–IV = ethmoturbinals II–IV; etr = ethmoturbinal recess; ft = frontoturbinal; it = interturbinal; lh = lamina horizontalis; lsc = lamina semicircularis; mt = marginoturbinal; mx = maxilla; mxt = maxilloturbinal; nph = nasopharyngeal duct; nt = nasoturbinal; pal = palatine.

Here, the development of the nasal turbinal of eulipotyphlans is presented. Presently, more than 500 species are assigned to the Order Eulipotyphla (Burgin et al. 2018). Regarding the body size, erinaceids weigh 50–1000 g (*Hylomys suillus* and *Erinaceus europaeus*), solenodontids weigh 1000 g and talpids weigh 10–400 g (*Neurotrichus gibbsii*, *Scaptonyx fusicaudus*, and *Desmana moschata*). Soricids are the smallest and weighs 2–100 g (*Suncus etruscus*, and *Suncus murinus*) (Symonds 2005; MacDonald 2009). Erinaceids and solenodontids are terrestrial, but soricids and talpids live in diverse environments (terrestrial, subterranean, and aquatic). Previously, where eulipotyphlans fall in the mammalian tree and phylogenetic relationships of the four families were disputed, the interrelationships are now mostly resolved (Sato et al. 2016, 2019; Springer et al. 2018; Upham et al. 2019), allowing detailed character evolution within the group.

Many studies have examined the eulipotyphlan turbinals (Paulli 1900c; Ganeshina et al. 1957; Sharma 1958; Gurtovoi 1966; Ioana 1970; Woehrmann-Repenning and Meinel 1977; Schmidt and Nadolski 1979; Kuramoto 1980; Söllner and Kraft 1980; Larochelle and Baron 1989; Maier 2002, 2020). However, almost all of them observed only adult specimens, this approach being highly problematic when examining the turbinal homology. Currently, the description of the fetal turbinal and the lamina is limited to a certain species: *E. europaeus* (Parker 1885; Fawcett 1918a; Michelsson 1922; Youssef 1971), *Hemiechinus auritus* (Youssef 1971), *Sorex araneus* (Parker 1885; de Beer 1929), *Suncus varilla* (Roux 1947), and *Talpa europaea* (Parker1885; Fischer 1901; Noordenbos1905; Fawcett 1918a). Using diffusible iodine-based contrast-enhanced computed tomography (diceCT) imaging, we describe the developmental stages of the nasal capsule and the cavity in five species of soricids and talpids for the first time. Histological sections of the erinaceids and solenodontids were reviewed from previous literature and used for comparison. Here, we propose revised turbinal homologies among eulipotyphlans and discuss the character evolution of the nasal turbinal.

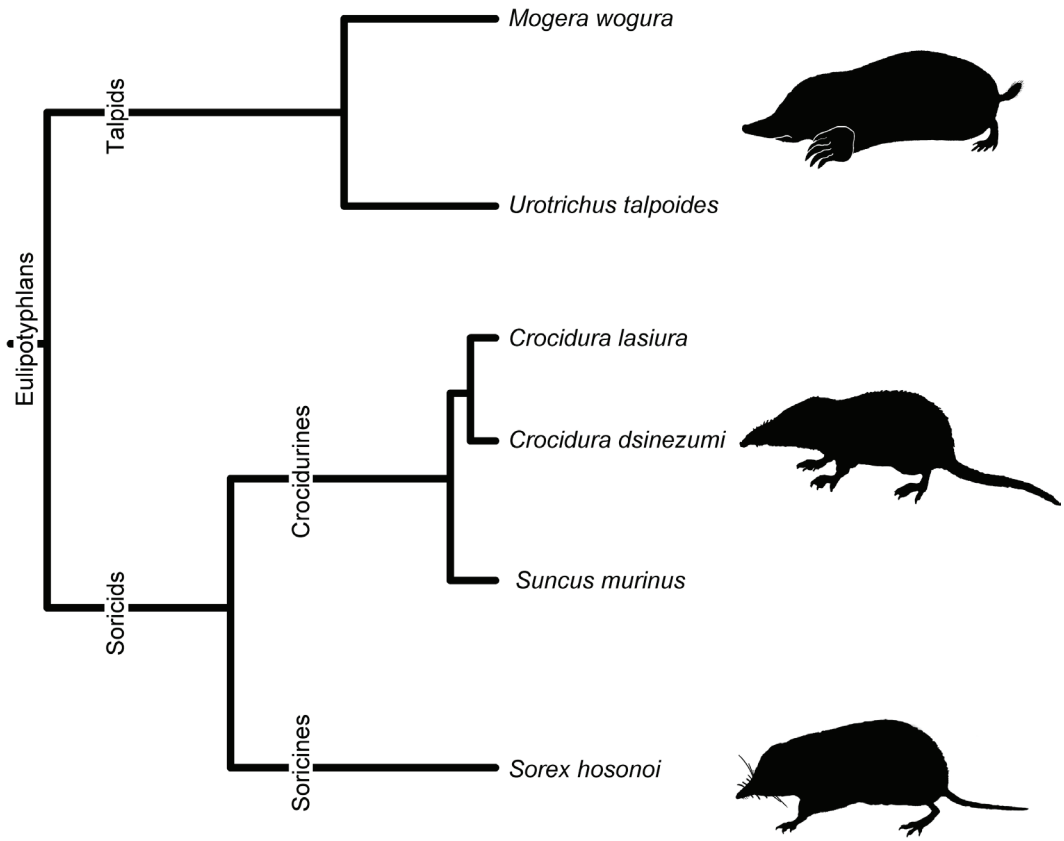

Figure 2. Phylogenetic relationships of eulipotyphlan species in this study. Phylogenetic framework is based on Ohdachi et al. (2004) and Sato et al. (2016, 2019).

Material and methods

We compared various developmental stages (fetus to adult) of talpids (two species) and soricids (four species) (Fig. 2). We investigated *Mogera wogura* and *Urotrichus talpoides* from talpids and *S. murinus*, *Crocidura dsinezumi*, *Crocidura lasiura*, and *Sorex hosonoi* from soricids. Developmental stages and measurements are listed in Table 2. All samples belong to the National Museum of Nature and Science and the University Museum of the University of Tokyo. As for fetuses, the exact day age of species, other than a few species of *S. murinus,* is unknown. Hence, we used the crown-rump length (CRL) and the external characteristics, based on Vogel (1972), Sterba (1977), and Barrionuevo et al. (2004) to infer the rough developmental stage. Based on the study that observed the initial protrusion of the turbinal (Parker 1885), we specified CRL 10 as the early stage. We specified those with approximately CRL 20 as late stage (the gestation length of *T. europaea*, *Crocidura russula*, and *Sorex etruscus* are commonly about 30 days) (Vogel 1972; Barrionuevo et al. 2004). Based on the size of the CRL (approximately CRL 15) and the external characteristics, it was presumed that the turbinals and laminae of the mid stage were more developed than those of the early stage. We also compared eulipotyphlans with *Sus scrofa*, *Felis catus*, and *Rousettus leschenaultii* which are reported previously in Ito et al. (2021) (Table 3).

Measurements were made using sliding calipers (N20, Mitutoyo, Japan). The samples were fixed and preserved with 70% ethanol solution. We followed the image enhancement techniques of a previous study (Gignac and Kley 2014; Gignac et al. 2016) and dipped the specimens with iodine-based solutions (1% iodine, I2KI in 99% ethanol solution). Staining duration was between 6 and 24 h in fetus and adult in 7 days depending on the size of the specimen.

We used a microCT scanner (InspeXio SMX-225CT, Shimadzu Co, Japan) with 110 kV source voltage and 100 mA source currents to create greyscale images of the specimens. Voxel size ranged from 8 to 35 µm. We used the dimensions of 2,048×2,048 pixels and 12-bit greyscale to reconstruct images. We manually reconstructed the cartilage and bones of the turbinals using Segmentation Editor Tool in Amira 5.3 (Visage Imaging, Berlin, Germany) for each specimen. The cartilaginous structures are often stained poorly by iodine-based solutions. However, they can be identified indirectly from the presence of surrounding connective tissues, such as the perichondria, which are readily stained with iodine-based solutions (Gignac et al. 2016). As depicted in Fig. 3, it was thus possible to distinguish ossified and cartilaginous structures from the surrounding structure.

The character states of the turbinals and lamina, such as the number, loss and gain, were mapped on to the phylogenetic tree (Ohdachi et al. 2004; Sato et al. 2016, 2019) to examine the evolutionary history of the nasal turbinals.

Table 2. Distribution and the number of turbinals and laminas of Eulipotyphla.

Species	Stage		CRL (mm)	Maxillo-turbinal	Lamina semi-circularis	Lamina horizontalis	Ethmo-turbinals	Fronto-turbinals	Inter-turbinal (between et I and et II)	Epiturbinal at et II	Specimen ID	Resolution (isotropic voxel size in mm)	References
Mogera wogura	early	gestation day 18	8.5	X	X	X	2	—	—	—	NSMT-M70506_a	0.006	this study
	mid	gestation day 22	12.8	X	X	X	3	1	1	—	NSMT-M70580_a	0.006	this study
	late	gestation day 26	22.0	X	X	X	3	1	1	—	NSMT-M70423_a	0.007	this study
	adult	—	NA	X	X	X	3	2	1	1	UMUT_TSCT21038	0.024	this study
Urotrichus talpoides	early	gestation day 18	6.4	X	X	X	2	—	—	—	UMUT_TSCT21048(236-1)	0.006	this study
	mid	gestation day 22	12.8	X	X	X	3	2	1	—	UMUT_TSCT21047	0.006	this study
	adult	—	NA	X	X	X	3	2	1	1	UMUT_TSCT21002	0.022	this study
Suncus murinus	early	gestation day 18	8.3	X	X	X	3	—	—	—	UMUT_TSCT21041	0.006	this study
	mid	gestation day 24	16.1	X	X	X	3	2	1	—	UMUT_TSCT21053	0.007	this study
	late	gestation day 29	19.8	X	X	X	3	2	1	—	UMUT_Suncus_KI02	0.007	Ito et al. 2021
	adult	—	NA	X	X	X	3	2	1	—	UMUT_KATS_835A	0.022	this study
Crocidura lasiura	early	gestation day 19	8.2	X	X	X	3	1	—	—	UMUT_TSCT21056	0.006	this study
Crocidura dsinezumi	mid	gestation day 23	12.8	X	X	X	3	2	1	—	UMUT_TSCT21049(107-1)	0.007	this study
	late	gestation day 26	18.1	X	X	X	3	2	1	—	UMUT_TSCT21046(141-1)	0.007	this study
	adult	—	NA	X	X	X	3	2	1	—	UMUT_TSCT21052	0.011	this study
Sorex hosonoi	early	gestation day 16	8.3	X	X	X	2	—	—	—	UMUT_TSCT21043	0.006	this study
	adult	—	NA	X	X	X	3	2	1	—	UMUT_TSCT21057	0.007	this study
Erinaceus europaeus	adult	—	NA	X	X	X	3	2	1	1	—	—	Parker 1885; Paulli 1900c; Fawcett 1918; Youssef 1971; Woehrmann-Repenning & Meinel 1977
Solenodon paradoxus	adult	—	NA	X	X	X	3	2	?	?	AMNH 28271, AMNH 28272	—	Wible 2008

Table 3. Distribution and the number of turbinals and laminas of Laurasiatheria.

Species	Stage		CRL	Maxillo-turbinal	Lamina semi-circularis	Lamina horizontalis	Ethmo-turbinals	Fronto-turbinals	Interturbinal (between et I and et II)	Epi-turbinal at et II	Specimen ID	Resolution (isotropic voxel size in mm)	References
Sus scrofa	mid	gestation day 28	17.9	X	X	X	2	1	—	—	UMUT_Pig_K013_KI_CRL18	0.011	Ito et al. 2021
	late	gestation day 40	42.4	X	X	X	4	3	X	X	UMUT_Pig_K76_KI_CRL42	0.016	Ito et al. 2021
	adult	—	—	X	X	X	6	4	X	X	—	—	Paulli 1900b
Felis catus	mid	gestation day 38	58.8	X	X	X	3	3	X	X	UMUT_Cat_K025_KI_CRL59	0.018	Ito et al. 2021
	late	gestation day 49	99.5	X	X	X	3	3	X	X	UMUT_Cat_K025_KI_CRL100	0.035	Ito et al. 2021
	adult	—	—	X	X	X	3	3	X	X	—	—	Paulli 1900c
Rousettus leschenaultii	early	gestation day 60 (CS 18)	7.4	X	X	X	1	—	—	—	VN17-366	0.009	Ito et al. 2021
	mid	gestation day 65 (CS 19)	9.6	X	X	X	3	1	—	—	VN17-357	0.012	Ito et al. 2021
	late	gestation day 85 (CS 23)	13.5	X	X	X	3	1	—	—	VN18-45	0.016	Ito et al. 2021
	adult	—	—	X	X	X	3	1	X	X	UMUT_KI19-001_sl41	0.031	Ito et al. 2021

Results

Marginoturbinal and atrioturbinal

The marginoturbinal was formed at the rostral-most dorsal side (dorsal to the naris) of the tectum nasi anterius from the early stage to adult in all eulipotyphlans (Figs 4A–G, 5A–J). The atrioturbinal was positioned on the caudal side of the marginoturbinal. The atrioturbinal was found at the ventral side of the nasal capsule from the early stage in all eulipotyphlans and almost no cartilaginous structure was formed within this turbinal in all eulipotyphlans. The maxilloturbinal was continuous with the caudal side of the atrioturbinal.

The marginoturbinal was also formed at the rostral-most dorsal side (dorsal to the naris) of the tectum nasi anterius from late stage of *Sus scrofa*, *Felis catus*, and from early to adult in *R. leschenaultii* (Fig. 6A–H). The atrioturbinal had few cartilaginous parts. The maxilloturbinal continued from the rostral side of the atrioturbinal.

We could not capture the clear image of the rostral-most turbinals of the early stage, such as the marginoturbinal and the atrioturbinal in all species with our CT imaging using the iodine-based solution. The thin cartilaginous structure made it difficult for us to distinguish the turbinal structure from other surrounding tissues. Especially the boundaries of turbinals were hard to observe in all species, such as between the marginoturbinal and the atrioturbinal and the atrioturbinal and the maxilloturbinal.

Maxilloturbinal

The maxilloturbinal of the talpids was already on the ventral side of the nasal capsule at the early stage (Fig. 4A, A-2, A-3, E, E-2, E-3). In the mid stage, the maxilloturbinal was not yet scrolled in both species (Fig. 4A, A-2, A-3, B, B-2, B-3, E, E-2, E-3, F, F-2, F-3). In the late stage of *M. wogura*, a slight depression was observed at the medial side of the caudal part of the maxilloturbinal (Fig. 4C, C-2, C-3). In the adult, the ossified plate was formed inside the maxilloturbinal in both species. All cartilage structures were ossified. The dorsal and ventral secondary lamellae of the maxilloturbinal are scrolled, and these scrolls became more prominent at the caudal ends (Fig. 4D-2, D-3, G-2, G-3).

The structure varied among soricids. *S. murinus*, *C. lasiura*, and *S. hosonoi* all formed the maxilloturbinal at the ventral side of the nasal capsule in the early stage (Fig. 5A, A-2, A-3, E, E-2, E-3, I, I-2, I-3). From the mid stage to the late stage of *S. murinus* and *C. dsinezumi*, the tip of the maxilloturbinal, which was dorsally scrolled, was not

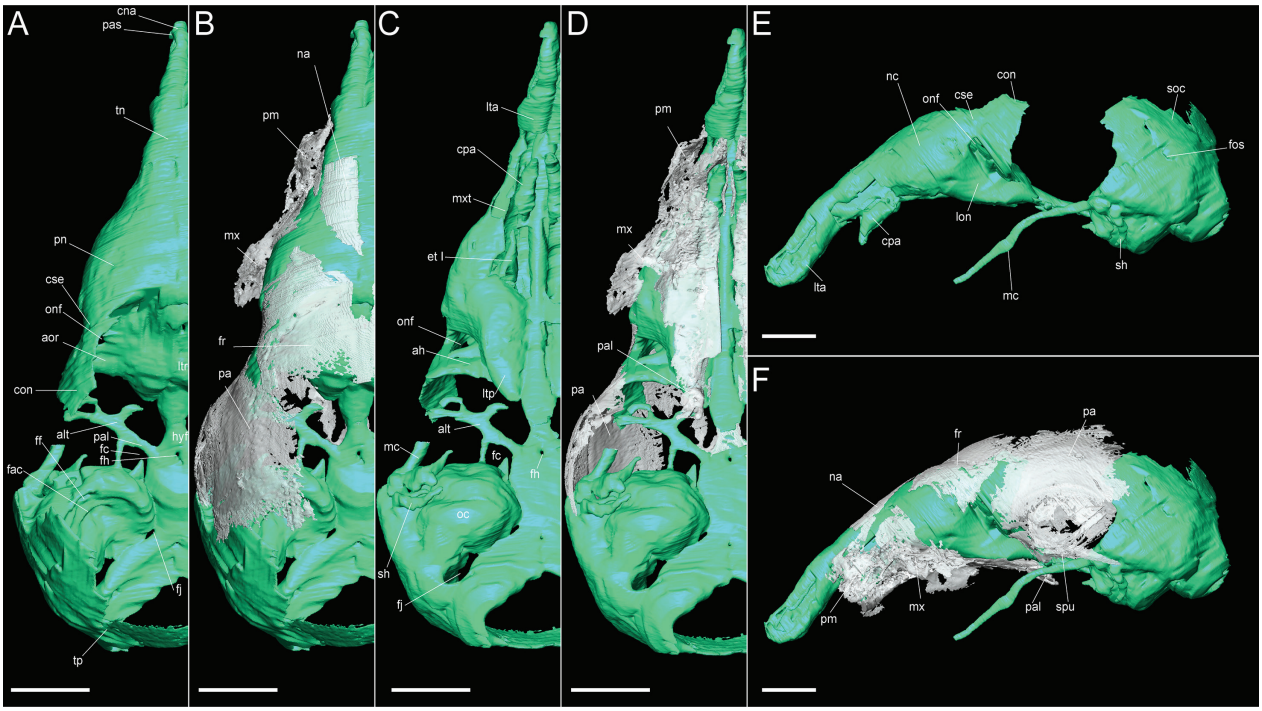

Figure 3. Virtual model of desmocranium (white) and chondrocranium (green) of *Suncus murinus* in the late stage. **A**, **B** Dorsal view of the left side; **C**, **D** ventral view of the left side; **E**, **F** lateral view of the left side; scale = 1 mm. Abbreviations: alt = ala temporalis; ah = ala hypochiasmatica; aor = ala orbit; bcf = basicranial fissure; con = orbitonasal commissure; con = commissura orbitonasalis; cpa = cartilago paraseptalis anterior; cse = sphenethmoid commissure; et I = ethmoturbinal I; fc = carotid foramen; ff = foramen of facial nerve; fh = hypophyseal fenestra; fj = foramen jugulare; fr = frontal; hyf = hypophyseal fossa; lon = laminas orbitonasalis; lta = lamina transversalis anterior; ltp = lamina transversalis posterior; ltr = lamina trabecularis; mc = Meckel's cartilage; mx = maxilla; mxt = maxilloturbinal; na = nasal; nc = nasalcapsule; oc = otic capsule; onf = orbitonasal fissure; onf = orbitonasal fissure; pa = parietal; pal = palatine bone; pal = palatinum; pm = premaxilla; pm = premaxilla; pn = paranasal cartilage; sh = stylohyal cartilage; soc = supraoccipital cartilage; squ = squamosal; tn = tectum nasi; tp = tectum posterius.

bifurcated, but only bulged (Fig. 5B, B-2, B-3, C, C-2, C-3, F, F-2, F-3, G, G-2, G-3). In the adult *S. murinus*, the dorsal and the ventral secondary lamellae were strongly scrolled and the dorsal secondary lamella produced an additional short branch (Fig. 5D, D-2). The maxilloturbinal of the adult *C. dsinezumi* bore two secondary lamellae (an unscrolled and almost straight dorsal lamella and a weakly-scrolled ventral lamella) (Fig. 5H, H-2). In the adult of *S. hosonoi*, the maxilloturbinal bore the dorsal and ventral secondary lamellae, but both lamellae were not scrolled (Fig. 5J, J-2).

The maxilloturbinal developed at the ventral side of the nasal capsule in all outgroup species. The maxilloturbinal formed the dorsal and ventral secondary lamellae in the mid stage in *S. scrofa*. In the late stage of *S. scrofa*, both secondary lamellae scrolled dorsally (Fig. 6A, A-2, B, B-2). In *F. catus*, the maxilloturbinal formed secondary lamellae, one dorsally and another ventrally, from the mid stage. In the late stage of *F. catus*, the scrolling of the ventral lamella became more prominent than the dorsal branch (Fig. 6C, C-2, D, D-2). In *R. leschenaultii*, a depression at the medial end of maxilloturbinal was observed. From the mid stage of *R. leschenaultii*, the maxilloturbinal formed the dorsal and ventral secondary lamellae. In the adult of *R. leschenaultii*, the two lamellae bore tertiary projections. The maxilloturbinal formed four lamellae in total (Fig. 6F, F-2, G, G-2, H, H-2).

Nasoturbinal

All the species observed in this study showed consistent characters. In the early stage of *M. wogura* and *U. talpoides*, a part of the nasoturbinal was protruding from the dorsal side to the ventral side near the nostrils (Fig. 4A, A-2, B, B-2, E, E-2, F, F-2). In the mid stage and the late stage of *M. wogura* and the mid stage of *U. talpoides*, the rostral nasoturbinal, which contained no cartilage inside, extended to the rostral direction (Fig. 4B-1, C-1, F-1). From the dorsal side of the tectum nasi anterius, the caudal nasoturbinal containing cartilage protruded ventrally and extended to the rostro-caudal direction (Fig. 4B, B-2, C, C-2, E, E-2, F, F-2). In the adults of *M. wogura* and *U. talpoides*, the nasoturbinal protruded caudally in the cavity of the outer nasal cartilages and extended in the rostro-caudal direction (Fig. 4D, D-1, G, G-1). We could not conclude whether the nasoturbinal in this part formed the cartilage inside the turbinal with our CT images after iodine staining. In the center of the bony nasal cavity, which was composed of the maxilla and nasal, and palatine bone, the nasoturbinal had a thin ossified plate inside.

In the early stage of *S. murinus* and *C. lasiura*, the protuberance was formed from the rostral side near the nostrils (Fig. 5A, A-1, E, E-1). However, it was difficult to judge from the CT image whether there was cartilage in this process. No protrusion of nasoturbinal was observed

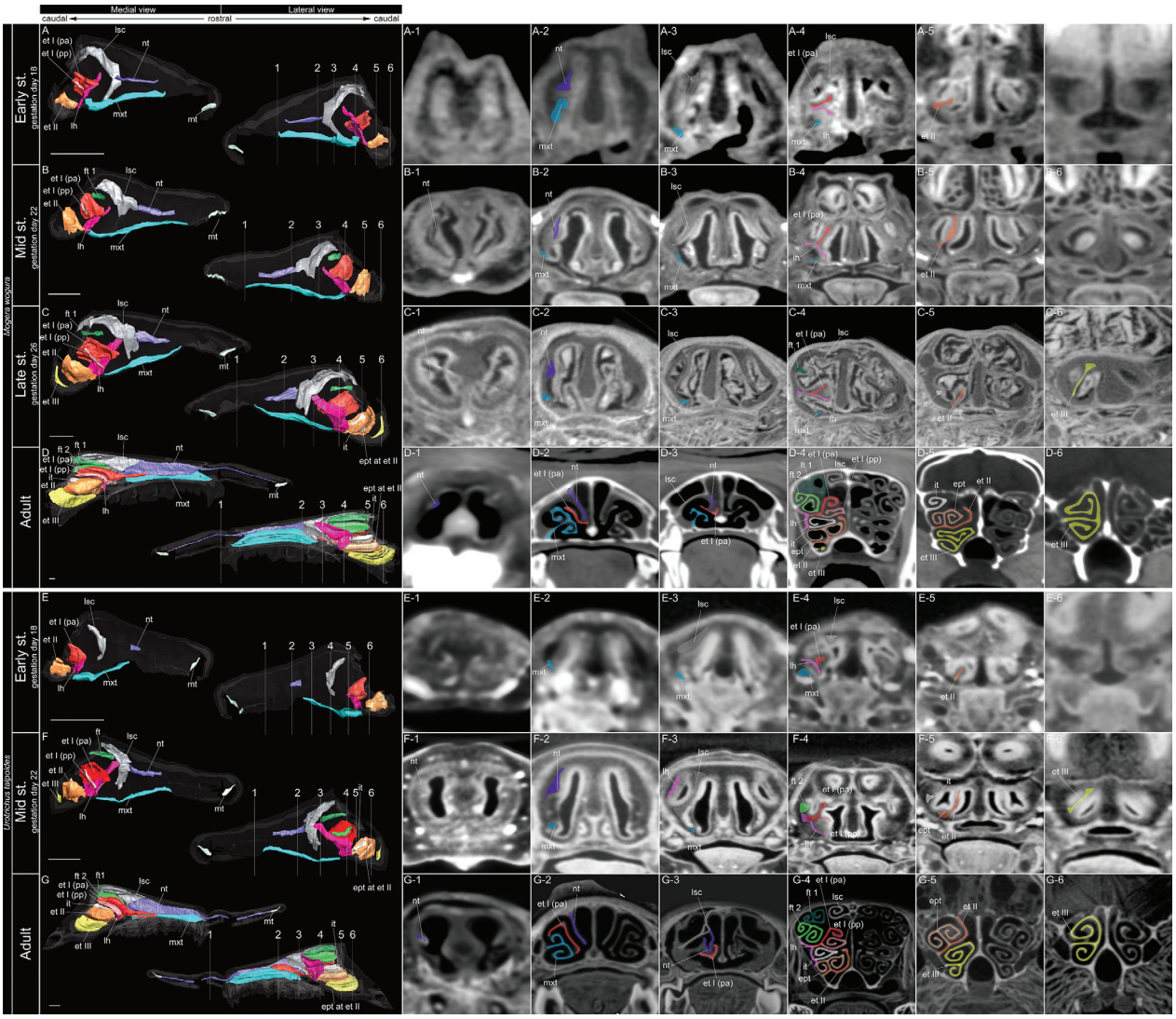

Figure 4. Coronal section and sagittal 3D views of µCT images of *Mogera wogura* and *Urotrichus talpoides*. **A**–**G** Show approximate location of section through the nasal capsule or nasal cavity. (A-1–6) Early stage fetus, (B-1–6) mid stage fetus, (C-1–6) late stage fetus, and (D-1–6) adult of *M. wogura*. (E-1–6) early stage fetus, (F-1–6) mid stage fetus, and (G-1–6) adult of *U. talpoides*. Scale bars: 1 mm. Abbreviations: ept = epiturbinal; et I (pa) = ethmoturbinal I pars anterior; et I (pp) = ethmoturbinal I pars posterior; et II–III = ethmoturbinal II–III; ft 1, 2= frontoturbinal 1, 2; it = interturbinal; lh = lamina horizontalis; lsc = lamina semicircularis; mt = marginoturbinal; mxt = maxilloturbinal; nt = nasoturbinal.

in the early stage of *S. hosonoi* (Fig. 5I). In the mid stage and the last late stage of *S. murinus* and *C. dsinezumi*, the rostral side of the nasoturbinal was only a process which the cartilage could not be observed inside. On their caudal side of the nasoturbinal, the cartilage was formed inside, protruding in the ventral direction and extending in the rostrocaudal direction (Fig. 5B, B-1, B-2, C, C-1, C-2, F, F-1, F-2, G, G-1, G-2). The nasoturbinal of the adult of soricids was roughly divided into two parts. One part of the nasoturbinal protruded dorsoventrally in the cavity of the outer nasal cartilages (Fig. 5D-1, H-1, J-1). The other part of the nasoturbinal was in the bony nasal cavity and protruded dorsoventrally. A thin ossified plate was formed inside this part of the nasoturbinal (Fig. 5D-2, H-2, J-2).

The nasoturbinal was rostrocaudally short and protruded from the inner wall of the rostral tectum nasi anterius in the mid stage of *S. scrofa* (Fig. 6A, A-1). The nasoturbinal of *S. scrofa* did not elongate rostrocaudally in the late stage (Fig. 6B, B-1). The nasoturbinal protruded from inner wall of the rostral tectum nasi anterius and its caudal side joined the rostral side of the lamina semicircularis in the mid stage of *F. catus* (Fig. 6C, C-2). The nasoturbinal was not observed from the early to late stages in *R. leschenaultii* (Fig. 6E–G). Nonetheless, a protrusion, presumably a nasoturbinal, was observed at the inner wall of the snout (Fig. 6H, H-1). This protrusion was not cartilaginous.

Lamina semicircularis

In the early stage of *M. wogura* and *U. talpoides*, the lamina semicircularis elongated in the dorsoventral direction and protruded medially (Fig. 4A, A-3, E, E-3). From the early to late stage of *M. wogura* and the early and the mid

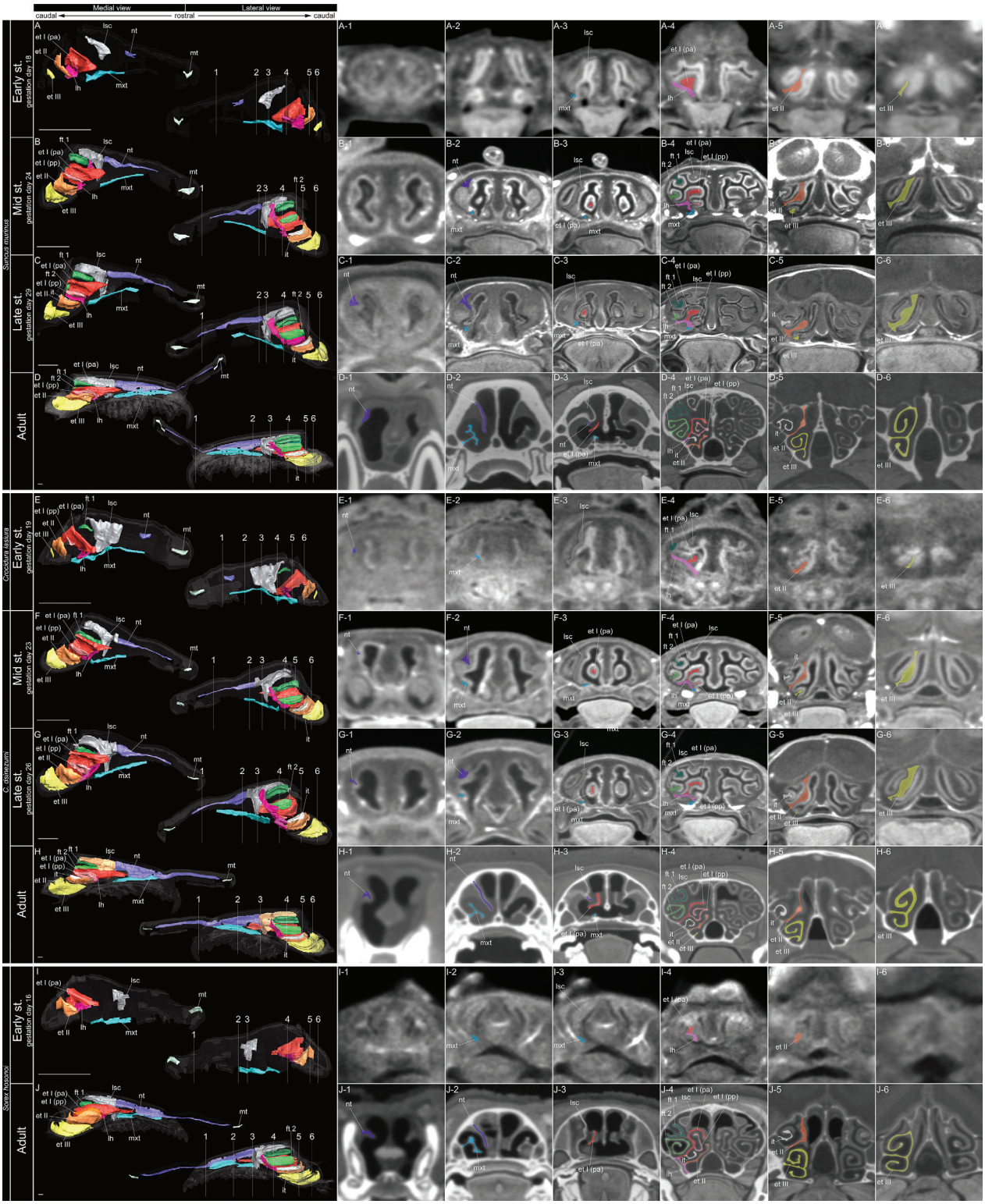

Figure 5. Coronal section and sagittal 3D views of µCT images of *Suncus murinus*, *Crocidura lasiura*, *C. dsinezumi*, and *Sorex hosonoi*. **A**–**J** show approximate location of section through the nasal capsule or nasal cavity. (A-1–6) Early stage fetus, (B-1–6) mid stage fetus, (C-1–6) late stage fetus, and (D-1–6) adult of *S. murinus*. (E-1–6) Early stage fetus of *C. lasiura*. (F-1–6) Mid stage fetus, (G-1–6) late stage fetus, and (H-1–6) adult of *C. dsinezumi*. (I-1–6) Early stage fetus, and (J-1–6) adult of *S. hosonoi*. Scale bars: 1 mm. Abbreviations: et I (pa) = ethmoturbinal I pars anterior; et I (pp) = ethmoturbinal I pars posterior; et II–III = ethmoturbinal II–III; ft 1, 2= frontoturbinal 1, 2; it = interturbinal; lh = lamina horizontalis; lsc = lamina semicircularis; mt = marginoturbinal; mxt = maxilloturbinal; nt = nasoturbinal.

stage of *U. talpoides*, the rostral side of the nasal capsule bridged the dorsal and ventral side. Then it expanded in the caudal direction to cover a part of the rostral side of the frontoturbinal and lamina horizontalis (Fig. 4A, A-3, B, B-3, E, E-3, F, F-3). In the adult *M. wogura* and *U. talpoides*, the rostral part of the nasal cavity had an os-

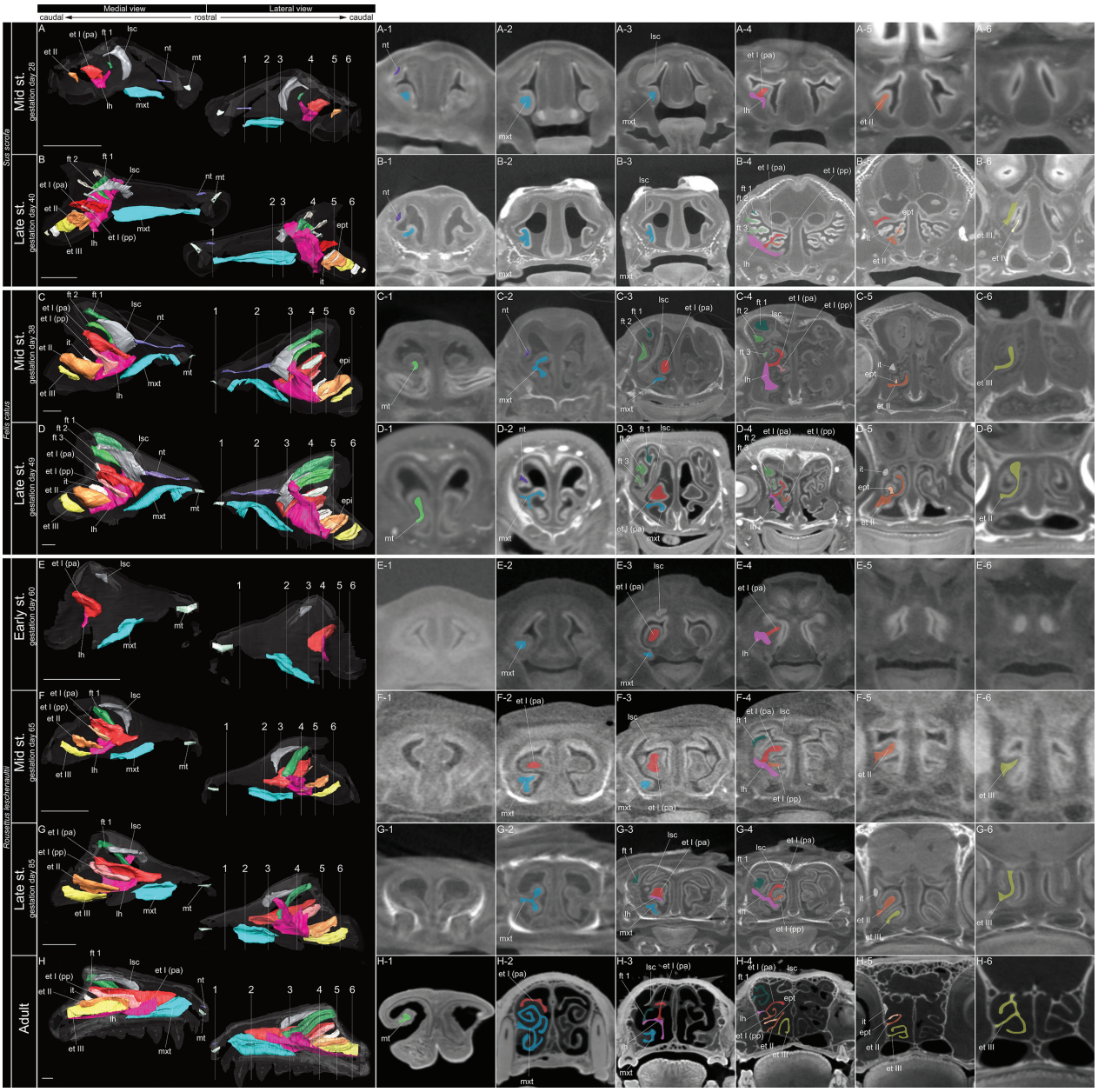

Figure 6. Coronal section and sagittal 3D views of µCT images of *Sus scrofa*, *Felis catus*, and *Rousettus leschenaultii*. **A**–**H** Show approximate location of section through the nasal capsule or nasal cavity. (A-1–6) Mid stage fetus and (B-1–6) late stage fetus of *Sus scrofa*. (C-1–6) Mid stage fetus and (D-1–6) late stage fetus of *Felis catus*. (E-1–6) Early stage fetus, (F-1–6) mid stage fetus, (G-1–6) late stage fetus, and (H-1–6) adult of *Rousettus leschenaultii*. Scale bars: 1 mm. Abbreviations: ept = epiturbinal; et I (pa) = ethmoturbinal I pars anterior; et I (pp) = ethmoturbinal I pars posterior; et II–III = ethmoturbinal II–III; ept = epiturbinal; ft 1–3= frontoturbinal 1–3; it = interturbinal; lh = lamina horizontalis; lsc = lamina semicircularis; mt = marginoturbinal; mxt = maxilloturbinal; nt = nasoturbinal.

sified structure inside the lamina that bridged the dorsal and lateral sides of the nasal cavity. On the caudal side of the nasal cavity, the lamina semicircularis was thinly ossified to surround the surface of this lamina. Further on the dorsal side, ossified lamellae emerged from the dorsal part of the lamina semicircularis and were single-scrolled outward (Fig. 4D, D-4, G, G-4).

In the early stage of *S. murinus*, *C. lasiura*, and *S. hosonoi*, the lamina semicircularis formed a dorsoventral expanding structure on the dorsal caudal side of the nasal capsule (Fig. 5A, E, I). From the mid stage to the late stage of *S. murinus* and *C. dsinezumi*, the lamina semicircularis bridged the dorsal and ventral sides in the rostral nasal capsule (Fig. 5B-3, C-3, F-3, G-3). In the caudal nasal capsule, the lamina semicircularis extended to the caud-medial side, spreading dorsoventrally over the rostral side of lamina horizontalis and the two frontoturbinals (Fig. 5B-3, C-3, F-3, G-3). In the mid stage of *S. murinus* and *C. dsinezumi*, an outwardly protruding process was formed on the dorsal side of the lamina semicircularis (Fig. 5B-4, F-4). This process was bent dorsally in the late stage of *S. murinus* (Fig. 5C-4). In the adults of *S. murinus*, *C. dsinezumi,* and *S. hosonoi*, the ossified part of the lamina semicircularis bridged the dorsal and ventral

sides on the rostral side of the nasal cavity (Fig. 5D-3, H-3, J-3). In the nasal cavity of adult soricids, the lamina semicircularis protruded in the dorsoventral direction. Furthermore, at the caudal side of the nasal cavity, the lamina semicircularis was thinly ossified and surrounded the surface (Fig. 5D, D-4, H, H-4, J, J-4). In the adults of *S. murinus* and *C. dsinezumi*, the lamina protruded outwards and scrolled to the dorsal side (Fig. 5D-4, H-4). In the adult of *S. hosonoi*, a laterally protruding process of the lamina semicircularis was observed on the dorsal side of the caudal nasal cavity (Fig. 5J-4).

In the mid stage of *S. scrofa*, the lamina semicircularis protruded from the inner wall of the dorsal side of nasal capsule (Fig. 6A, A-3). In the late stage of *S. scrofa,* the rostral side of the lamina semicircularis bridged the dorsal and the lateral side of the nasal capsule, and the caudal side of the lamina semicircularis extended medially on the dorsal side of the nasal capsule (Fig. 6B, B-3). In themid stage of *F. catus*, the rostral side of the lamina semicircularis bridged the dorsal and the lateral side of the nasal capsule (Fig. 6C, C-3, D, D-3). In the early stage of *R. leschenaultii*, the lamina semicircularis protruded on the dorsal side of the nasal capsule (Fig. 6 E, E-3). From the mid- to the late stages of *R. leschenaultii*, the lamina semicircularis projected laterally and transversally (Fig. 6F, F-3, G, G-3). In the adult, the lateral tip was slightly scrolled dorsally (Fig. 6H, H-3).

Lamina horizontalis

The lamina horizontalis of *M. wogura* and *U. talpoides* protruded from the inner lateral wall of the nasal capsule in the early stage, joining the ventral side of ethmoturbinal I pars anterior (Fig. 4A, E). Within *M. wogura* from mid to adult, and *U. talpoides* of mid and adult, the lamina horizontalis consistently extended from the inner wall of the nasal capsule in the direction of latero-medial, rostro-caudal and caudo-rostral. In the mid stage of *M. wogura*, the dorsal side of the lamina horizontalis was joined only to the ethmoturbinal I pars anterior (Fig. 4B, B-4). In the mid stage *U. talpoides*, the dorsal side of the lamina horizontalis fused with the ventral side of the ethmoturbinal I pars anterior, the ethmoturbinal I pars posterior, and the interturbinal (Fig. 4F, F-4). In the late stage of *M. wogura*, the dorsal side of the lamina horizontalis was fused with the ventral side of the ethmoturbinal I pars anterior and the ethmoturbinal I pars posterior (Fig. 4C). In the adult of both species, two frontoturbinals and ethmoturbinal I pars anterior and ethmoturbinal I pars posterior, and interturbinal, ethmoturbinal II were combined from the dorsal side of the lamina horizontalis (Fig. 4D, G).

A similar tendency was observed for soricids as for talpids. In the early stage of *S. murinus* and *C. lasiura*, the lamina horizontalis was already fused with the ventral side of the ethmoturbinal I and II and protruded from the inner lateral wall of the nasal capsule to the cavity (Fig. 5A, A-4, E, E-4). From the mid stage to the adult of *S. murinus*, the lamina horizontalis fused with the ventral sides of the two frontoturbinals, the ethmoturbinal I pars anterior and the ethmoturbinal I pars posterior, and interturbinal and expanded inwards to enclose them (Fig. 5B–D). In the mid stage of *C. dsinezumi*, the lamina horizontalis was associated with the ventral sides of the two frontoturbinals, the ethmoturbinal I pars anterior, and the ethmoturbinal I pars posterior (Fig. 5F). From the late stage of *C. dsinezumi*, the lamina horizontalis additionally expanded inwards to wrap around them (Fig. 5G). In the adult of *S. murinus*, *C. dsinezumi* and *S. hosonoi*, the lamina horizontalis expanded inwards, fusing with the ventral sides of the two frontoturbinals, the ethmoturbinal I pars anterior, ethmoturbinal I pars posterior, and the interturbinal (Fig. 5D, H, J).

In the mid stage of *S. scrofa*, the lamina horizontalis protruded transversally from the inner lateral wall of the nasal capsule, joining with the ventral side of the ethmoturbinal I pars anterior (Fig. 6A, A-4). In the late stage, it joined the ventral side of the ethmoturbinal I pars posterior, ethmoturbinal II, three frontoturbinals, and the interturbinal (Fig. 6B, B-4). From the mid- to late stage of *F. catus*, the lamina horizontalis protruded transversally from the inner lateral wall, joining the ventral side of the ethmoturbinal pars anterior, ethmoturbinal pars posterior, ethmoturbinal II and three frontoturbinals and the interturbinal (Fig. 6C, C-4, D, D-4). In the early stage of *R. leschenaultii*, the lamina horizontalis protruded from the inner lateral wall, joining the ventral side of the ethmoturbinal I pars anterior (Fig. 6E, E-4). From the mid stage to the adult, the lamina horizontalis projected mediolaterally from the inner lateral wall of the nasal capsule, joining the ethmoturbinal pars anterior, ethmoturbinal II, ethmoturbinal III and two frontoturbinals (Fig. 6F, F-4, G, G-4, H, H-4).

Frontoturbinal

The frontoturbinals were not observed in the early stage of *M. wogura* and *U. talpoides* (Fig. 4A, E). In the mid stage of *M. wogura*, the frontoturbinal 1 protruded from the inner wall on the dorsal side of the nasal capsule (Fig. 4B). The late stage of *M. wogura* and the mid stage of *U. talpoides* had two frontoturbinals (the frontoturbinal 1 on the dorsal side and the frontoturbinal 2 on the ventral side) protruding from the dorsal inner wall of the nasal capsule without branching off (Fig. 4C, F). In the adults of *M. wogura* and *U. talpoides*, the two frontoturbinals were on the dorsal side of the nasal cavity. The rontoturbinal 1 diverged inwards and outwards, scrolling on both internal and external lamellae. The frontoturbinal 2 diverged dorsally and ventrally, forming scrolled lamellae (Fig. 4D, D-4, G, G-4).

No frontoturbinal protrusions were observed in the early stages of *S. murinus*, and *S. hosonoi* (Fig. 5A, A-4, I, I-4). From the mid stages of *S. murinus* and *C. dsinezumi*, two frontoturbinals (the frontoturbinal 1 on the dorsal side and the frontoturbinal 2 on the ventral side) protruded from the dorsal inner wall of the nasal capsule (Fig. 5B, B-4, F, F-4). The inner tip of each frontoturbi-

nal was greatly swollen (Fig. 5B, B-4, C, C-4, F, F-4, G, G-4). In the adults of *S. murinus* and *C. dsinezumi*, both frontoturbinals scrolled inwards and outwards (Fig. 5D, D-4, H, H-4). In *S. hosonoi*, the frontoturbinal 1 formed the dorsal and ventral lamellae which scrolled dorsally and ventrally (Fig. 5J, J-4). The frontoturbinal 2 formed inward and outward lamellae; the outward lamella did not scroll, while the inward one scrolled (Fig. 5J, J-4).

In the mid stage of *S. scrofa*, the frontoturbinal 1 protruded slightly from the inner wall of the dorsal side of the nasal capsule (Fig. 6A). In the late stage, two additional frontoturbinals (the frontoturbinal 2 and the frontoturbinal 3) appeared in the dorsal side of the nasal (Fig. 6B, B-4). From the mid stage of *F. catus*, three frontoturbinals protruded from the inner wall of the dorsal side of the nasal capsule and fused with the dorsal side of the lamina horizontalis already (Fig. 6C, C-4, D, D-4). From the mid stage to adult of *R. leschenaultii*, a frontoturbinal protruded from the inner wall of the dorsal side of the nasal capsule and fused dorsally to the lamina horizontalis (Fig. 6F, F-4, G, G-4, H, H-4). In adults, the frontoturbinal 1 branched off and scrolled (Fig. 6H, H-4).

Ethmoturbinal I pars anterior

The ethmoturbinal I pars anterior of talpids (*M. wogura* and *U. talpoides*) protruded in the latero-medial and caudo-rostral directions from the inner lateral wall of the nasal capsule, fusing with the dorsal side of the lamina horizontalis at the early stage. (Fig. 4A, A-4, E, E-4). From the early stage to the adult of *M. wogura* and the early, mid and adult stages of *U. talpoides*, this turbinal was the largest of all ethmoturbinals (Fig. 4A–G). From the early stage of *M. wogura* and from the mid stage of *U. talpoides*, this turbinal had the ethmoturbinal I pars posterior branched from the ventral side (Fig. 4A, A-4, F, F-4). In addition, from the mid stage of both species, the rostral part of the ethmoturbinal I pars anterior protruded towards the nostrils (Fig. 4B, F). In the adult, the rostral part of this turbinal formed a caudo-rostral elongated structure. (Fig. 4D, G).

Fusing with the dorsal side of the lamina horizontalis, the ethmoturbinal I pars anterior of soricids, like the talpids, protruded from the inner lateral wall of the nasal capsule in latero-medial and caudo-rostral directions already at the early stage (Fig. 5A, A-4, E, E-4, I, I-4). From the early stage to the adult, the ethmoturbinal I pars anterior was always the largest among all ethmoturbinals in soricids. (Fig. 5A–J). From the mid stage to the adult stages of *S. murinus* and *C. dsinezumi*, the rostral side of the ethmoturbinal I pars anterior elongated towards the naris (Fig. 5B–D, F–H). From the mid stage, the ethmoturbinal I pars anterior of *S. murinus* and *C. dsinezumi* showed a gradual ventral curve (Fig. 5B, B-4, F, F-4). Furthermore, from this stage, another branch, the ethmoturbinal I pars posterior, protruded from the ventral base of the ethmoturbinal I pars anterior (Fig. 5B, B-4, F, F-4).

In the late stage of both species, the curve of the ethmoturbinal I pars anterior which bent to the ventral side became stronger, and the innermost tip of this turbinal was swollen (Fig. 5C, C-4, G, G-4). In the adults of *S. murinus*, *C. dsinezumi*, and *S. hosonoi*, the ethmoturbinal I pars anterior formed two secondary lamellae (inside and outside), and the inner lamella bent at an acute angle to the ventral side. On the other hand, the outer lamella did not scroll or even bend.

From the mid stage of *S. scrofa*, the ethmoturbinal I pars anterior protruded from the inner lateral wall of the nasal capsule, fusing with the dorsal side of the lamina horizontalis (Fig. 6A, A-4). In the mid stage of *S. scrofa*, the ethmoturbinal I pars posterior diverged from the ventral side of the ethmoturbinal I pars anterior (Fig. 6B, B-4). From the mid stage of *F. catus*, the ethmoturbinal I pars anterior protruded from the inner lateral wall of the the nasal capsule, joining the dorsal side of the lamina horizontalis. The ethmoturbinal I pars posterior branched from the ventral side of the ethmoturbinal I pars anterior already in the mid stage of *F. catus* (Fig. 6C, C-4). The inner end of the ethmoturbinal I pars anterior was bifurcated at the late stage of *F. catus* (Fig. 6C, C-4, D, D-4). In *R. leschenaultii*, the ethmoturbinal I pars anterior protruded from the inner lateral wall of the nasal capsule, fusing with the dorsal side of the lamina horizontalis at the early stage (Fig. 6E, E-4). From the mid stage of *R. leschenaultii*, the ethmoturbinal I pars anterior projected towards the rostral side and was located on the dorsal side of the maxilloturbinal (Fig. 6F–H). Furthermore, the ethmoturbinal I pars posterior diverged from the ventral side of the ethmoturbinal I pars anterior (Fig. 6F–H). The ethmoturbinal I pars anterior was the largest turbinal among all ethmoturbinals in all stages in all species of the outgroup.

Ethmoturbinal I pars posterior

In *M. wogura*, the ethmoturbinal I pars posterior projected from the ventral side of the ethmoturbinal I pars anterior from the early stage (Fig. 4A, A-4). In the early stage of *U. talpoides*, the ethmoturbinal I pars posterior was not branched (Fig. 4E). In the mid- and late stages of *M. wogura* and the mid stage of *U. talpoides*, the ethmoturbinal I pars posterior extended towards the septum nasi (Fig. 4B, B-4, C, C-4, F, F-4). In the adult of both species, the ethmoturbinal I pars posterior scrolled to the dorsal side, and the rostral side of this turbinal joined the dorsal side of the lamina horizontalis (Fig. 4D, D-4, G, G-4).

In the early stage of *C. lasiura*, the ethmoturbinal I pars posterior was observed at the base of the ethmoturbinal I pars anterior (Fig. 5E). In *S. murinus*, the ethmoturbinal I pars posterior was observed from the mid stage (Fig. 5B, B-4). The medial tip of the ethmoturbinal I pars posterior in the mid and late stages of *S. murinus* and *C. dsinezumi* was swollen (Fig. 5B, B-4, C, C-4, F, F-4, G, G-4). In the adult of *S. murinus* and *C. dsinezumi*, the ethmoturbinal I pars posterior bore two secondary lamellae. The dorsal lamella scrolled strongly outwards, and the ventral lamella did not scroll. In the adult of *S. hosonoi*, the ethmoturbinal I pars posterior did not branch off, but only formed a dorsally directed weak curve.

In *S. scrofa*, the ethmoturbinal I pars posterior protruded from the ventral side of the ethmoturbinal I pars anterior in the late stage and the ventral side of the ethmoturbinal I pars posterior fused with the dorsal side of the lamina horizontalis (Fig. 6A, A-4, B, B-4). In *F. catus*, the ethmoturbinal I pars posterior protruded from the ventral side of the ethmoturbinal I pars anterior and fused with the dorsal side of the lamina horizontalis from the mid stage (Fig. 6C, C-4, D, D-4). From the mid stage of *R. leschenaultii*, the ethmoturbinal I pars posterior protruded from the ventral side of the ethmoturbinal I pars anterior and fused with the dorsal side of the lamina horizontalis (Fig. 6F, F-4, G, G-4, H, H-4).

Turbinals in the ethmoturbinals recessus

In *M. wogura* and *U. talpoides*, the ethmoturbinal II already protruded from the inner lateral wall of the ventral side of the nasal capsule at the early stage (Fig. 4A, A-5, E, E-5). In the mid stages of *M. wogura* and *U. talpoides*, the ethmoturbinal II extended medio-dorsally from the ventral inner wall and joined the dorsal inner wall in the caudal nasal capsule (Fig. 4B, B-5, F, F-5). From the late to the adult stages in *M. wogura* and the mid to the adult stage in *U. talpoides*, the ethmoturbinal II extended towards the septum nasi and curved dorsally then joined the inner wall of the nasal caspule or the nasal cavity (Fig. 4C, C-5, D, D-5, F, F-5, G, G-5). The ethmoturbinal II did not scroll in both species (Fig. 4C, C-5, D, D-5, F, F-5, G, G-5). From the late stage to the adult of *M. wogura* and from the mid stage to the adult of *U. talpoides*, the epiturbinal protruded from the dorsal side of ethmoturbinal II (Fig. 4C, C-5, D, D-5, F, F-5, G, G-5). In the adult of both species, the epiturbinal at the ethmoturbinal II, formed the lateral and medial lamellae, and both lamellae scrolled ventrally (Fig. 4D, D-5, G, G-5).

From the late stage of *M. wogura* and from the mid stage of *U. talpoides*, the ethmoturbinal III protruded from the nasal wall (Fig. 4C, C-6, F, F-6). In the adult of both species, the ethmoturbinal III bore the secondary lamellae; the dorsal lamella scrolled ventrally, and the ventral lamella scrolled dorsally. In both species, the dorsal scroll of the ethmoturbinal III was more prominent than the ventral scroll (Fig. 4D, D-6, G, G-6). Moreover, the interturbinal protruded from the inner lateral wall of nasal capsule in the late stage of *M. wogura* and in the mid stage of *U. talpoides* (Fig. 4C, C-5, F, F-5). In the adult, the interturbinal protruded medially from the inner wall and turned, extending laterally. Furthermore, the tip scrolled ventrally (Fig. 4D, D-5, G, G-5).

The ethmoturbinal II protruded ventrally from the inner wall of the nasal capsule in all soricids already at the early stage (Fig. 5A, A-5, E, E-5, I, I-5). From the mid to late stages of *S. murinus* and *C. dsinezumi*, the ethmoturbinal II extended ventromedially and weakly curved dorsally at the ventral side of the nasal capsule (Fig. 5B, B-5, C, C-5, E, E-5, F, F-5). In the adults of *S. murinus*, *C. dsinezumi* and *S. hosonoi*, the ethmoturbinal II extended to the septum nasi and curved at an obtuse angle then joined the dorsal side of the nasal cavity (Fig. 5D, D-5, H, H-5, J, J-5). The ethmoturbinal II did not scroll and project any lamella as the epiturbinal of all sorcids species (Fig. 5D-4, D-5, H-4, H-5, J-4, J-5).

In *S. murinus* and *Crocidura dsinezum*, the ethmoturbinal III was a minor cartilaginous protrusion at the early stage (Fig. 5A, A-6, E, E-6). The ethmoturbinal III was not observed in the early stage of *S. hosonoi* (Fig. 5 I, I-6). From the mid to the late stages of *S. murinus* and *C. dsinezumi* and late stage of *S. murinus*, the ethmoturbinal III extended medially from the inner wall of the nasal capsule and joined dorsally to the dorsal side of the inner wall. The lateral and medial side of ethmoturbinal III was swollen (Fig. 5B, B-6, C, C-6, F, F-6, G, G-6). In the adults of *S. murinus*, *C. dsinezumi*, and *S. hosonoi*, the ethmoturbinal III formed the ventral and dorsal secondary lamellae, which are scrolled. The dorsal lamella scrolled ventrally at the rostral side of the ethmoturbinal III, and the ventral lamella scrolled dorsally at the caudal side of the ethmoturbinal III (Fig. 5D-5, D-6, H, H-6, J, J-6).

The interturbinal was not observed in all soricids species in the early stage (Fig. 5A, E, I). It protruded from the inner wall of the nasal capsule between the ethmoturbinal I and II in the mid stages of *S. murinus* and *C. dsinezumi* (Fig. 5B, B-5, F, F-5). In the adult of *S. murinus*, the interturbinal formed the medial and lateral secondary lamellae; the medial secondary lamella strongly scrolled ventrally, and the lateral secondary lamella did not scroll (Fig. 5D-5). The lateral branch disappeared completely at the caudal side of the nasal cavity (Fig. 5D-5). In the adult of *C. dsinezumi*, the interturbinal did not bear the secondary lamellae, but only scrolled medially (Fig. 5H-5). In the adult of *S. hosonoi*, the rostral side of the interturbinal protruded from the lateral side of the ethmoturbinal I pars anterior and the caudal side of the interturbinal protruded from the inner wall of the nasal cavity (Fig. 5J-4, J-5).

From the mid stage of *S. scrofa*, the ethmoturbinal II protruded from the inner lateral wall of the ventral side of the nasal capsule, and the ridge of the epiturbinal was located ventrally to the ethmoturbinal II (Fig. 6A, A-5). In the mid stage of *F. catus*, the ethmoturbinal II projected from the inner lateral wall of the ventral side of the nasal capsule. The ridge of the epiturbinal was located at the dorsal side of the ethmoturbinal II already in this stage (Fig. 6C, C-5). From the mid stage of *R. leschenaultii*, the ethmoturbinal II protruded from the inner lateral wall of the ventral side of the nasal capsule (Fig. 6F, F-5). While the epiturbinal was not observed in the fetal stages of *R. leschenaultii*, the epiturbinal was seen at the dorsal side of the ethmoturbinal II in the adult (Fig. 6H-4, H-5).

From the late stage, the ethmoturbinal III and the ethmoturbinal IV protruded dorsally from the inner wall of the ventral side of the nasal capsule in *S. scrofa* (Fig. 6B, B-6). In the mid stage of *F. catus,* the ethmoturbinal III protruded dorsally from the inner wall of the ventral side of the nasal capsule. In the late stage, the medial tip bulged medially (Fig. 6D, D-6). In the mid stage of *R. leschenaultii,* the ethmoturbinal III protruded from the in-

ner wall of the ventral side of the nasal capsule, extending dorsally. In the adult, the ethmoturbinal III bore the dorsal and ventral secondary lamellae (Fig. 5F, F-6).

From the late stage of *S. scrofa* and from the mid stage of *F. catus*, the interturbinal protruded from the inner lateral wall of the nasal capsule between the ethmoturbinal I pars posterior and ethmoturbinal II (Fig. 6B, B-5, C, C-5). In *R. leschenaultii*, the interturbinal was not found in the fetal stage, but protruded from the nasal cavity between the ethmoturbinal I pars posterior and the ethmoturbinal II in the adult (Fig. 6E–H, H-5).

Discussion

Talpids

In talpines, other than *M. wogura* and *U. talpoides*, which are discussed here, there have been many reports on the turbinal of *T. europaea* using both adults and fetuses. The turbinals of adult specimens were described by Ganeshina et al. (1957), Ioana (1970), and Woehrmann-Repenning and Meinel (1977). Among these studies, Ganeshina et al. (1957) and Woehrmann-Repenning and Meinel (1977) showed some detailed coronal sections of the nasal cavity. The nasal cavity of *T. europaea* resembles that of *M. wogura* and *U. talpoides* observed in this study (Ganeshina et al. 1957; Woehrmann-Repenning and Meinel 1977) (Fig. 4). Woehrmann-Repenning and Meinel (1977) showed the ethmoturbinal I that split into two with a caudal section of *T. europaea*. In addition, *T. europaea* also showed the ethmoturbinal II which protrudes from the inner lateral nasal wall and bends dorsally (see in their fig. 4e). Hence, like *M. wogura* and *U. talpoides*, *T. europaea* has the interturbinal that protrudes from the inner lateral nasal wall between the ethmoturbinal I pars posterior and the ethmoturbinal II and the epiturbinal that protrudes from the dorsal side of the ethmoturbinal II (Woehrmann-Repenning and Meinel 1977). Martinez et al. (2020) did not identify the turbinals in their study, but instead distinguished them solely on olfactory and respiratory functions. Their detailed CT images of the coronal section and histological sections of *T. europaea* which they presented show the interturbinal that protrudes from the inner lateral nasal wall between the ethmoturbinal I pars posterior and the ethmoturbinal II and the epiturbinal that protrudes dorsally from the ethmoturbinal II.

Parker (1885), Fischer (1901), Noordenbos (1905), and Fawcett (1918) described the fetal stages of *T. europaea.* Parker (1885) showed detailed coronal sections of two fetal stages (the size of the fetuses are 15.9 mm and 19.1 mm from the snout to the root of the tail; Parker used a unique method to measure specimens). From his caudal section of the nasal capsule, we were able to observe the structure which protrudes from the inner wall to the septum nasi and extends horizontally and the protrusion from the dorsal region of the structure. Moreover, the structure that extends horizontally in Parker's figure resembles the structure and the position of the lamina horizontalis of the early to mid stages of *M. wogura* and *U. talpoides* (Fig. 4A-4, B-4, E-4, F-4). Therefore, we suggest that these structures are homologous. In addition, the caudal section of the nasal capsule showed the protruding turbinal structure that extends ventrodorsally. In the smaller fetus, Parker (1885) called this a rudimentary middle turbinal (plate 23, fig. 6) In the larger fetus, the cartilaginous structure thickened mediolaterally. The resemblance of the structure and the position indicates that this turbinal and the ethmoturbinal II of *M. wogura* and *U. talpoides* of the early and mid stages are homologous. Nonetheless, the interturbinal that protrudes from the inner lateral nasal wall between the ethmoturbinal I pars posterior and the ethmoturbinal II and the epiturbinal that protrudes dorsally from the ethmoturbinal II that Woehrmann-Repenning and Meinel (1977) and Martinez et al. (2020) described in adult *T. europaea* were not observed in the coronal sections of the two fetuses presented by Parker (1885). Parker (1885) presented several fetuses, but did not show any figures with detailed turbinal structures other than the two which we discussed. Hence, the protrusion of the interturbinal and the epiturbinal at the ethmoturbinal II started after the stages that Parker (1885) illustrated. Thus, the description of the turbinals of talpids was chiefly carried out, based on *T. europaea.* No-one has ever described the nasal capsule and the turbinals of other fetal talpids.

To our knowledge, only studies on scalopine *Condylura cristata* and talpine *D. moschata* show detailed descriptions of turbinal structures, other than *T. europaea* (Allen 1882; Ganeshina et al. 1957; Martinez et al. 2020) for talpids. Allen (1882) included *C. cristata* as an outgroup species in the study on chiropterans, but did not show any detailed figures. He also stated that *C. cristata* has three ethmoturbinals and four other turbinals (frontoturbinal or interturbinal; Allen 1882). Martinez et al. showed the CT sections and the three-dimensional turbinal image of adult *C. cristata* (Martinez et al. 2020). Their caudal CT image showed the largest turbinal which split into two (Martinez et al. 2020). The structure seen in this image resembles what we observed in *M. wogura* and *U. talpoides*; hence, we can identify them as the ethmoturbinal I pars anterior and the ethmoturbinal I pars posterior. Moreover, the study illustrated the turbinal that protruded from the lateral wall of the nasal cavity and extended dorsally. This also resembles the structure in *M. wogura* and *U. talpoides*; hence, we identify it as the ethmoturbinal II. The interturbinal protruded from the inner wall between the ethmoturbinal I pars posterior and the ethmoturbinal II made a dorsal single scroll. In the section, the epiturbinal is slightly visible in dots on the dorsal side of the ethmoturbinal II. In his image, the epiturbinal is slightly visible on the dorsal side of ethmoturbinal II. Based on these factors, we can assume that the four turbinals, other than the ethmoturbinal within the ethmoturbinal recess which Allen (1882) identified, are most probably the dorsally positioned two frontoturbinals, interturbinal, and the epiturbinal at the dorsal region of the ethmoturbinal II. Furthermore, Ganeshina et al. (1957) and Martinez et al. (2020) observed the turbinal structure of talpine *D.*

moschata. Martinez et al. (2020) showed the CT images of the rostral and the caudal side of the nasal cavity. The CT image that showed the turbinals of the ethmoturbinal recess of *D. moschata* in Martinez et al. (2020) exhibited the ethmoturbinal I pars anterior and the ethmoturbinal I pars posterior, and the ethmoturbinal II that protruded from the ventral side of the lateral nasal wall and extended dorsally. Their figure also presented the interturbinal that protruded from the inner lateral nasal wall between the ethmoturbinal I pars posterior and the ethmoturbinal II and the epiturbinal that protruded from the dorsal side of the ethmoturbinal II. Hence, the turbinal structure of the ethmoturbinal recess of *D. moschata* is the same as that of the rest of the talpid species.

The maxilloturbinal of *T. europaea* (Ganeshina et al. 1957; Woehrmann-Repenning and Meinel 1977; Martinez et al. 2020) and *C. cristata* (Martinez et al. 2020) resembles that of *M. wogura* and *U. talpoides* in terms of structure and size (forming the two secondary lamellae, one extending dorsally, while the other extending ventrally). A previous study showed that among other talpids, the relative surface area of the respiratory turbinals (nasoturbinal and maxilloturbinal) of the amphibious species (such as *D. moschata* and *Galemys pyrenaicus*) is larger than in the terrestrial species. An inverted pattern was found for the olfactory turbinals (ethmoturbinal, frontoturbinal, and interturbinal) (Martinez et al. 2020). The rostral section of *D. moschata* indicates that the maxilloturbinal structure is rather similar to the structure seen in other talpids species observed previously (form the two secondary lamellae and each scrolls).

Similar to the early and mid stages of *M. wogura* and *U. talpoides* in this study, the maxilloturbinal of the two fetal stages of *T. europaea* presented by Parker (1885) does not bear the secondary lamellae. Fischer (1901) who observed the chondrocranium of *T. europaea* also stated that the maxilloturbinal is undeveloped. It is most likely that the development of the secondary lamellae in the maxilloturbinal occurs in the fetal stage right before birth or the early neonatal period.

Soricids

Soricids include subfamilies, such as crocidurines, myosoricines, and soricines (Willows-Munro and Matthee 2009). The studies of myosoricines include the description of the snout by Maier (2020) and the quantification of the turbinal surface area by Martinez et al. (2020). The turbinal structure is mainly described using crocidurines and soricines; crocidurines have been studied by many authors using various adult species, such as *C. suaveolens* (Ganeshina et al. 1957; Ioana 1970), *S. murinus* (Sharma 1958; Kuramoto 1980), *C. russula* (Woehrmann-Repenning and Meinel 1977; Schmidt and Nadolski 1979; Söllner and Kraft 1980) and *C. leucodon* (Ioana 1970; Söllner and Kraft 1980). The position and the structure of the turbinal described in the previous studies showed resemblance with our observation of *S. murinus* and *C. dsinezumi* (Fig. 5D, H). The ethmoturbinal I of crocidurines splits into two: the ethmoturbinal I pars anterior directing dorsally and the ethmoturbinal I pars posterior directing ventrally. Moreover, the ethmoturbinal I is the largest of all turbinals. The ethmoturbinal II extends ventrodorsally. The ethmoturbinal III forms two secondary lamellae and each structure scrolls. Furthermore, the interturbinal protrudes from the inner lateral nasal wall between the ethmoturbinal I pars posterior and the ethmoturbinal II and forms two secondary lamellae, and each secondary lamella of the interturbinal scrolls. The epiturbinal protrusion from the dorsal side of the ethmoturbinal II has not been found.

To our knowledge, Roux (1947) is the only study that described the fetal crocidurine with the observation of the development of *S. varilla*. The author showed the section of the nasal capsule with only an CRL 18 mm fetus. The turbinal structure of *S. varilla* presented by Roux (1947) resembles that of the mid and late stages of *S. murinus* and *C. dsinezumi* (Fig. 5B, C, F, G). The fetus of *S. varilla* (Roux 1947) has the ethmoturbinal I pars posterior, which is the ventral one of the bifurcated ethmoturbinal I, and II, which extends from the ventral side of the inner nasal wall to the dorsal side. One interturbinal is found between these turbinals. There is no epiturbinal on the dorsal side of the ethmoturbinal II (Roux 1947).

There have been many studies on the turbinal structure of adult soricines, such as *S. araneus* (Paulli 1900c; Ärnbäck Christle-Linde 1907; Ganeshina et al. 1957; Ioana 1970; Woehrmann-Repenning and Meinel 1977; Söllner and Kraft 1980; Parker 1885; Maier 2002, 2020), *Sorex hoyi* (Ganeshina et al. 1957), *Neomys fodiens* (Ioana 1970; Söllner and Kraft 1980; Maier 2002, 2020), *Sorex minutus* (Söllner and Kraft 1980), and *Blarina brevicauda*, *Sorex cinereus*, *Sorex fumeus*, and *Sorex palustris* (Larochelle and Baron 1989). The number of turbinals is consistent (Woehrmann-Repenning and Meinel 1977; Söllner and Kraft 1980; Larochelle and Baron 1989). The structure of the turbinals within the ethmoturbinal recess of *S. hosonoi* observed in this study and that of the species of previous studies were also consistent. As for the structure of the ethmoturbinal recess of soricines, the ethmoturbinal I splits into two with the ethmoturbinal I pars anterior extending dorsally and the ethmoturbinal I pars posterior extending ventrally; the ethmoturbinal I is the largest of all turbinals. The ethmoturbinal II extends ventrodorsally. The ethmoturbinal III bears two secondary lamellae and scrolls caudally (Ärnbäck Christle-Linde 1907; Ganeshina et al. 1957; Woehrmann-Repenning and Meinel 1977; Söllner and Kraft 1980; Larochelle and Baron 1989).

The turbinal found between the ethmoturbinal I pars posterior and the ethmoturbinal II in soricines is rather different from the interturbinal, which is found between the ethmoturbinal I pars posterior and the ethmoturbinal II in crocidurines (Larochelle and Baron 1989). While the structure seen in soricines made a dorsal single scroll, the interturbinal of crocidurines bear two secondary lamellae, both lamellae scrolling ventrally (Larochelle and Baron 1989). We also observed the difference in the structure of the turbinal between the ethmoturbinal I pars posterior and the ethmoturbinal II among *S. hosonoi* and

S. murinus (Fig. 5D-5, J-5). There have been disagreements over the identification of the turbinal between the ethmoturbinal I pars posterior and the ethmoturbinal II. Larochelle and Baron (1989) identified this turbinal as the accessory of the ethmoturbinal I since the caudal side of the turbinal lamellae is from the root of the ethmoturbinal I. On the other hand, Woehrmann-Repenning and Meinel (1977) and Söllner and Kraft (1980) identified it as the interturbinal that protrudes from the inner lateral nasal wall to the cavity space. At the moment, the observation of the adult turbinals does not allow us to resolve the problem of identification.

De Beer (1929) described fetal soricine using *S. araneus*. For a fetus with the size of CRL 11 mm, he illustrated a sole protrusion at the inner lateral nasal wall between the ethmoturbinal I pars posterior and ethmoturbinal II. While de Beer did not refer to this protrusion, we regard this structure as a primordium of the interturbinal before the cartilage penetrates from the inner lateral nasal wall. Parker (1885) illustrated a short protrusion filled with cartilaginous structure at the inner lateral nasal wall between the ethmoturbinal I pars posterior and ethmoturbinal II in the coronal section of the neonate of *S. araneus* (10–12 day old) (plate 30) (Supplementary Fig. 1). He did not name each turbinal in the study and only stated the short protrusion as "middle turbinal". The region of the protrusion of the "middle turbinal" is identical to that of the "protrusion" described by de Beer in the fetus of CRL 11 mm. We were not able to observe a turbinal structure between the ethmoturbinal I pars posterior and ethmoturbinal II in the early stage of *S. hosonoi* (Fig. 5I-5). Nonetheless, the position and the structure of the interturbinal observed in the late stages of *S. murinus* and *C. dsinezumi* are identical to that of the short protruding turbinal illustrated in the neonate of Parker 1885; hence, identifying the protrusion of de Beer (1929) and the short protrusion of Parker (1885) as interturbinals is compelling (Fig. 5C-5, G-5). By comprehending the observation of de Beer's fetal *Sorex* and the neonate of Parker (1885), together with the observation of the development of fetal crocidurines in this study, we support the claim of Ganeshina et al. (1957), Woehrmann-Repenning and Meinel (1977), and Söllner and Kraft (1980) that the turbinal between the ethmoturbinal I pars posterior and the ethmoturbinal II in soricines is the interturbinal rather than the identification of Larochelle and Baron (1989) as the accessory of the ethmoturbinal I.

Some studies claim that the maxilloturbinal of *N. fodiens* does not bear the secondary lamellae, but scrolls dorsally and the maxilloturbinal of *S. araneus* bears two secondary lamellae (Söllner and Kraft 1980; Larochelle and Baron 1989); nonetheless, their observations are limited to several histological sections. In fact, Maier showed that the maxilloturbinal of *N. fodiens* forms three lamellae (two dorsally and one ventrally) using serial sections (Maier 2002; Maier 2020). Additionally, Woehrmann-Repenning and Meinel (1977) indicated that the maxilloturbinal of *S. araneus* forms three lamellae (one dorsally and two ventrally). Several studies showed that the maxilloturbinal of *S. murinus* forms two lamellae (Sharma 1958; Kuramoto 1980; Larochelle and Baron 1989), but these assertions were based on only a few sections. In this study, we indicate that the maxilloturbinal of *S. murinus* forms three lamellae using serial CT sections (Fig. 5D-2). Researchers are prone to misjudgements when identifying turbinals using only a few sections. To accurately comprehend the turbinal structure, we have to make sections in which we can identify all turbinal lamellae (a very fortunate phenomenon); the alternative solution is to observe serial sections or CT images that show continuous turbinal structures.

Furthermore, several authors reported that the maxilloturbinal does not form any lamellae in fetal soricids, while it bears two to three lamellae in the adult as described here and in other studies (de Beer 1929; Roux 1947) (Fig. 5D-2, H-2, J-2). The maxilloturbinal does not form the secondary lamellae in postnatal (10–12 day-old) *S. araneus* described by Parker (1885). Hence, it is highly likely that the maxilloturbinal of soricids forms the secondary lamellae in the postnatal period.

Other members in eulipotyphlans

Researchers have looked closely into the turbinal structure of *E. europaeus* for erinaceids (Parker 1885; Paulli 1900c; Fawcett 1918; Ganeshina et al. 1957; Gurtovoi 1966; Woehrmann-Repenning and Meinel 1977). Paulli (1900c), Ganeshina et al. (1957), Gurtovoi (1966), and Woehrmann-Repenning and Meinel (1977) showed the section of adult *E. europaeus*. The ethmoturbinal I protrudes from the inner lateral nasal wall and splits into the dorsal pars anterior and the ventral pars posterior. The ethmoturbinal II extends from the ventral to the dorsal side. The ethmoturbinal III forms two secondary lamellae and each scrolls. The turbinal structure and the position exhibited in the previous studies are similar to those of talpids and soricids which we observed. The coronal section of adult *E. europaeus* indicates that the interturbinal protrudes from the inner lateral nasal wall between the ethmoturbinal I pars posterior and the ethmoturbinal II (Paulli 1900c; Ganeshina et al. 1957; Gurtovoi 1966; Woehrmann-Repenning and Meinel 1977) (Supplementary Fig. 2). Moreover, Paulli (1900c), Gurtovoi (1966), and Woehrmann-Repenning and Meinel (1977) observed the epiturbinal that protruded from the ethmoturbinal II (Supplementary Fig. 2).

To accurately conclude that the interturbinal and the epiturbinal of erinaceids are homologous structures to those of talpids and soricids, we have to examine their development. Nonetheless, the study on the erinaceid turbinal structure is very limited. To our knowledge, two species have been the subject of research: *E. europaeus* (Parker 1885; Fawcett 1918; Mishelsson1922) and *H. auritus* (Youssef 1971). Among these, coronal sections are provided by Parker (1885) with a fetus with a body length of 31.8 mm and Youssef (1971) with a fetus with a head length of 7.5–8.5 mm. Unfortunately, their fetuses are rather small such that only a few turbinals and laminae (most likely the lamina horizontalis, ethmoturbinal I,

lamina semicircularis, and the frontoturbinal 1) are observed within the ethmoturbinal recess. As the development of the interturbinal and the epiturbinal at the ethmoturbinal II is not observed in these fetuses, it is necessary to observe various developmental stages to identify the turbinals of erinaceids. According to the previous turbinal studies on adult *E. europaeus*, the interturbinal protrudes from the inner lateral nasal wall between the ethmoturbinal I and the ethmoturbinal II within the ethmoturbinal recess, and the epiturbinal protrudes from the dorsal side of the ethmoturbinal II. Paulli (1900c), Fawcett (1918), and de Beer (1929) stated that the structure of the nasal cavity of erinaceids does not vary between Talpidae and Sorex. Nonetheless, as the epiturbinal protrudes from the ethmoturbinal II, the structure of erinaceids shows a close resemblance with talpids rather than soricids (Table 2).

Moreover, previous descriptions show that *E. europaeus* has a multi-branching and ventrally enlarged maxilloturbinal (Parker 1885; Ganeshina et al. 1957; Gurtovoi 1966; Woehrmann-Repenning and Meinel 1977). However, all fetuses of Parker (1885), Fawcett (1918), and Mishelsson (1922) do not indicate any bifurcations. Similar to talpids and soricids, we do not know when the maxilloturbinal erinaceids bifurcates.

The nasoturbinal of adult *E. europaeus* is rostrocaudally elongated, and it is also formed at the snout region (Ganeshina et al. 1957; Gurtovoi 1966; Woehrmann-Repenning and Meinel 1977).

As for solenodontids, a destroyed skull of adult *Solenodon paradoxus* exhibits the turbinals of the nasal cavity (Wible 2008). Wible (2008) showed the ethmoturbinal I–III in the ethmoturbinal recess (Table 2). Nonetheless, he did not describe the interturbinal and the epiturbinal at the ethmoturbinal II; this is most likely because he could not perceive the detailed nasal structure from the damaged skull, including the presence or the absence of the interturbinal and the epiturbinal.

The maxilloturbinal of adult *S. paradoxus* enlarges at the ventral side of the nasal cavity with many lamellae (Wible 2008).

The nasoturbinal is rostrocaudally elongated. Maier (2020) showed that the external nasal cartilages of *S. paradoxus* enlarges (Maier 2020). While it is uncertain as Maier (2020) did not describe the nasoturbinal in the snout, if *S. paradoxus* had the nasoturbinal in the snout as in mammals in general, their nasoturbinal would be longer rostrocaudally than the nasoturbinal observed by Wible (2008) from the dry skull.

Character Evolution of Turbinals in Talpids and Soricids

Here, we show the molecular phylogenetic tree of eulipotyphlans (Fig. 7). The turbinal bones are very thin and fragile. A few studies described the turbinals, based on fossils; however, there is a limit to how far we can understand the turbinal structure based on fossils (Maier 1983; Maier and Ruf 2014; Ruf et al. 2014, 2021). Even if a fossil of a common ancestor of all eulipotyphlans species were to be found, the possibility of observing the turbinal structure would be quite low. As the turbinal structures cannot be comprehended through fossils, estimating these from the living species is effective for understanding the evolution of turbinals.

Eulipotyphlans belongs to boreoeutherians, which also includes euarchontoglirans (dermopterans, lagomorphans, primates, rodentians, and scandentians) and laurasiatherians (carnivorans, cetartiodactylans, pholidotans, perissodactylans, and chiropterans) (Waddell et al. 1999). The turbinal structures in some of these groups are listed in Table 4, following previous studies.

Here we summarise the structure of the turbinal and lamina of eulipotyphlans (Fig. 7). The number of the ethmoturbinal and the structure of the nasoturbinal and lamina semicircularis are consistent among the species of eulipotyphlans. The number of the ethmoturbinal of talpids and soricids which we observed is the same (ethmoturbinal I–III) (Table 2). Previous studies of the turbinal of eulipotyphlans also showed that the number of the ethmoturbinal is between I–III (Ganeshina et al. 1957; Gurtovoi 1966; Ioana 1970; Woehrmann-Repenning and Meinel 1977; Söllner and Kraft 1980; Larochelle and Baron 1989; Wible 2008). We can predict that the common ancestor of eulipotyphlans had ethmoturbinal I–III (Fig. 7).

Moreover, the nasoturbinal extends rostrocaudally and protrudes dorsoventrally within the nasal cavity (Figs 4, 5). The rostral side of the lamina semicircularis fused to the caudal side of the nasoturbinal and the caudal side of the lamina semicircularis expands dorsoventrally (Ganeshina et al. 1957; Gurtovoi 1966; Ioana 1970; Woehrmann-Repenning and Meinel 1977; Söllner and Kraft 1980; Larochelle and Baron 1989; Wible 2008) (Figs 4, 5).

The structure of the ethmoturbinal recess and the maxilloturbinal varies among groups in eulipotyphlans. As for the turbinals within the ethmoturbinal recess, erinaceids have the interturbinal that protrudes from the inner lateral nasal wall between the ethmoturbinal I pars posterior and the ethmoturbinal II and the epiturbinal that protrudes from the ethmoturbinal II as reported in laurasiatherians other than eulipotyphlans (no previous research on solenodontids) (Paulli 1900c; Ganeshina et al. 1957; Gurtovoi 1966; Woehrmann-Repenning and Meinel 1977; Wible 2008). Talpids also have the interturbinal that protrudes from the inner lateral nasal wall between the ethmoturbinal I pars posterior and the ethmoturbinal II and the epiturbinal that protrudes from the ethmoturbinal II (Fig. 4D-4, D-5, G-5, G-4). Hence, we consider this "interturbinal that protrudes from the inner lateral nasal wall between the ethmoturbinal I pars posterior and the ethmoturbinal II and the epiturbinal that protrudes from the ethmoturbinal II" as the basal structure of the ethmoturbinal recess (Fig. 7). In soricids, this study showed that the epiturbinal is not formed at the ethmoturbinal II (Fig. 5D-5, H-5, J-5). Hence, the turbinal modification (the absence of the epiturbinal at the ethmoturbinal II) at the ethmoturbinal recess of eulipotyphlans occurred in soricids (Fig. 7).

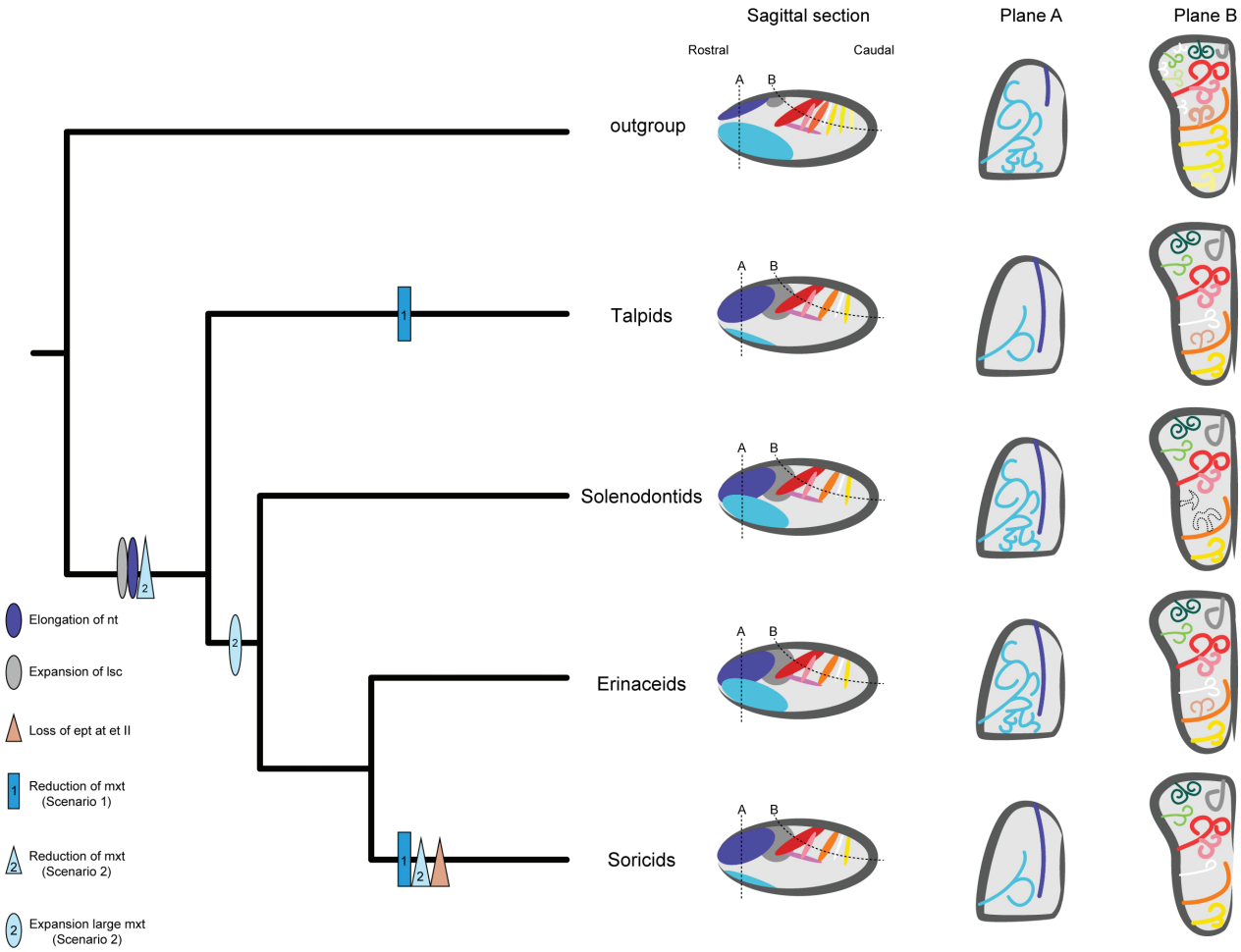

Figure 7. Inferred evolutionary history of the nasal structures. Nasoturbinal (purple); maxilloturbinal (light blue); frontoturbinal (green, light green); lamina semicircularis (grey); lamina horizontalis (pink); ethmoturbinal I pars anterior (red); ethmoturbinal I pars posterior (light coral); ethmoturbinal II (orange); ethmoturbinal III (yellow); ethmoturbinal IV (light yellow); epiturbinal (chocolate); interturbinal (white); unknown turbinal (broken line).

The maxilloturbinal of erinaceids (Parker 1885; Woehrmann-Repenning and Meinel 1977) and solenodontids (Wible 2008) is large at the ventral side with more than three lamellae (multi-branching) like other laurasiatherians. On the other hand, previous studies and this study show that the maxilloturbinal of talpids and soricids forms two or three lamellae (Figs 4D-2, G-2, 5D-2, H-2, J-2) (Ganeshina et al. 1957; Gurtovoi 1966; Woehrmann-Repenning and Meinel 1977; Söllner and Kraft 1980; Larochelle and Baron 1989). While the lamellae of the maxilloturbinal of talpids and soricids exhibits a slight difference in number, they are similar in a development pattern such that their "maxilloturbinal do not form the lamellae even at the late stage just before birth" (Figs 4C-2, F-2, 5C-2, G-2). Moreover, the maxilloturbinal do not form the lamellae in the new bone of *E. europaeus* (Parker 1885).

Therefore, two scenarios for the evolution of the maxilloturbinal of eulipotyphlans can be suggested: 1) The maxilloturbinal is reduced independently in talpids and soricids. Based on the maximum parsimony method, in this scenario, we believe that the multi-branching maxilloturbinal, which was obtained by the common ancestor of laurasiatherians, reduced independently in the ancestor of talpids and soricids (Fig. 7). 2) The maxilloturbinal reduced in the common ancestor of eulipotyphlans. This scenario is supported by the commonality of the developmental processes of the maxilloturbinal in eulipotyphlans. The reduced maxilloturbinal later bore the lamellae and enlarged in the common ancestor of erinaceids, solenodontids, and soricids. Moreover, the maxilloturbinal of soricids was again reduced (Fig. 7). The second scenario would have more character-state changes and can be problematic. In turbinal evolution, compared with forming a brand new turbinal, it is rather popular to increase or decrease the number of lamellae at the peripheral region to increase or decrease the size of the maxilloturbinal; hence, this change can be seen in various lineages. The change in size can easily occur in turbinal evolution. Although not parsimonious as the first scenario, the second scenario cannot be eliminated as the size of the turbinal is evolutionary labile. To confirm this hypothesis, we must observe the course of development in the maxilloturbinal from the fetus (when the maxilloturbinal starts bearing the secondary lamellae) to adult in each group of eulipotyphlans.

Table 4. Turbinate structure of boreoeutherians.

Taxonomic Groups		Maxilloturbinal	Lamina horizontalis	Ethmoturbinals (et)	Frontoturbinals (ft)	Interturbinal (between et I and et II)	Epiturbinal at et II	Nasoturbinal	References
euarchontoglirans	scandentians	folded (*Ptilocercus*, *Tupaia*)	protruding from the inner lateral wall of the nasal wall (*Ptilocercus*, *Tupaia*)	et I–III (*Ptilocercus*, *Tupaia*)	ft = 2 (*Ptilocercus*, *Tupaia*)	present	present	reduced (*Ptilocercus*, *Tupaia*)	Zeller 1987; Ruf et al. 2015
	dermopterans	folded (*Cynocephalus*, *Galeopterus*)	protruding from the inner lateral wall of the nasal wall (*Cynocephalus*, *Galeopterus*)	et I–IV (*Cynocephalus*, *Galeopterus*)	ft = 2 (*Cynocephalus*, *Galeopterus*)	present (*Cynocephalus*, *Galeopterus*)	absent (*Cynocephalus*, *Galeopterus*)	No description	Smith and Rossie 2008; Lundeen and Kirk 2019
	primates	single scrolled (*Callithrix*, *Cebuella*, *Gorilla*, *Homo*, *Lemur*, *Pan*, *Papio*, *Pongo*) double scrolled (*Alouatta*, *Eulemur*, *Daubentonia*, *Loris, Microcebus*)	absent (*Callithrix*, *Homo*, *Hylobates*, *Macaca*, *Papio*, *Saimiri*) protruding from the inner lateral wall of the nasal wall (*Daubentonia*, *Eulemur*, *Lemur, Microcebus*)	et I (*Callithrix*, *Cebuella*) et I–II (*Hylobates*, *Macaca*, *Papio*, *Saimiri*) et I–III (*Daubentonia*, *Eulemur*, *Homo*, *Lemur, Microcebus*)	absent (*Callithrix*, *Homo*, *Papio*) ft = 1 (*Microcebus*) ft = 3 (*Daubentonia*)	absent (*Homo*) present (*Daubentonia, Microcebus*) present (*Daubentonia*)	absent (*Homo*, *Macaca, Microcebus*) present (*Daubentonia*)	reduced (*Cebut*, *Cercopithecus*, *Homo*, *Hylobates*, *Lagothrix*, *Macaca*, *Papio*) elongated rostrocaudally (*Daubentonia*, *Eulemur, Microcebus*)	Paulli 1900c; Negus 1958; Moore 1981; Maier 1993; Smith and Rossie 2006; Smith et al. 2007, 2011, 2015; Maier and Ruf 2014
	lagomorphans	branching	protruding from the inner lateral wall of the nasal wall	et I–II (*Ochotona*, *Romerolagus*) et I–III (*Lepus*, *Oryctolagus*, *Poelagus*, *Pronolagus*, *Sylvilagus*) et I–IV (Caprolagus)	ft = 2	present	absent	elongated rostrocaudally and dorsoventrally	Negus 1958; Ruf 2014
	rodentians	double scrolled folded	protruding from the inner lateral wall of the nasal wall	et I–III	ft = 2	present	present	elongated rostrocaudally and dorsoventrally	Negus 1958; Martinez et al. 2018; Ruf 2004, 2020; Ruf et al. 2021; Smith and Bonar 2022

Taxonomic Groups		Maxilloturbinal	Lamina horizontalis	Ethmoturbinals (et)	Frontoturbinals (ft)	Interturbinal (between et I and et II)	Epiturbinal at et II	Nasoturbinal	References
laurasiatherians	eulipotyphlans	branching (*Erinaceus*, *Solenodon*) double scrolled (*Crocidura*, *Mogera*, *Sorex*, *Talpa*, *Urotrichus*)	protruding from the inner lateral wall of the nasal wall	et I–III (*Crocidura*, *Erinaceus*, *Mogera*, *Sorex*, *Talpa*, *Urotrichus*)	ft = 2 (*Crocidura*, *Erinaceus*, *Mogera*, *Solenodon*, *Sorex*, *Talpa*, *Urotrichus*)	present (*Crocidura*, *Erinaceus*, *Mogera*, *Sorex*, *Talpa*, *Urotrichus*)	present (*Erinaceus*, *Mogera*, *Talpa*, *Urotrichus*)	elongated rostrocaudally and dorsoventrally (*Crocidura*, *Erinaceus*, *Mogera*, *Solenodon*, *Sorex*, *Talpa*, *Urotrichus*)	Negus 1958; Parker 1885; Ganeshina et al. 1957; Gurtovoi 1966; Woehrmann-Repenning and Meinel 1977; Söllner and Kraft 1980; Larochelle and Baron 1989; Wible 2008
	chiropterans	folded (*Cynopterus*, *Rousettus*) reduced (*Aselliscus*, *Hipposideros*, *Myotis*, *Rhinolophus*, *Vespertilio*)	absent (*Myotis*, *Vespertilio*) protruding from the inner lateral wall of the nasal wall (*Aselliscus*, *Cynopterus*, *Hipposideros*, *Rhinolophus*, *Rousettus*)	et I–III (*Cynopterus*, *Myotis*, *Pteropus*, *Rousettus*, *Vespertilio*) et I–IV (*Aselliscus*, *Hipposideros*, *Rhinolophus*)	ft = 1 (*Aselliscus*, *Cynopterus*, *Hipposideros*, *Myotis*, *Rhinolophus*, *Rousettus*, *Vespertilio*)	absent (*Aselliscus*, *Hipposideros*, *Myotis*, *Rhinolophus*, *Vespertilio*) present (*Cynopterus*, *Rousettus*, *Pteropus*)	absent (*Aselliscus*, *Hipposideros*, *Myotis*, *Rhinolophus*, *Vespertilio*) present (*Cynopterus*, *Rousettus*, *Pteropus*)	reduced (*Cynopterus*, *Rousettus*) present (*Aselliscus*, *Hipposideros*, Myotis, *Rhinolophus, Vespertilio*)	Frick 1954; Giannini et al. 2012; Ito et al. 2021
	cetartiodactylans	double scrolled (*Bison*, *Sus*)	protruding from the inner lateral wall of the nasal wall	et I–III (*Capra*) et I–IV (*Bos*, *Camelus*, *Cervus*, *Ovis*) et I–VI (*Sus*)	number unknown (ft and it are mixed)	absent	present	reduced	Paulli 1900b; Negus 1958; Hillenius 1994
	perissodactylans	folded (*Tapirus*) single scrolled (*Equus*) double scrolled (*Rhinoceros*)	protruding from the inner lateral wall of the nasal wall	et I–V (*Equus*, *Rhinoceros*) et I–VI (*Tapirus*)	number unknown (ft and it are mixed)	present	present	reduced	Paulli 1900b; Negus 1958; Hillenius 1994; Witmer et al. 1999; Kupke et al. 2016
	pholidotans	branching	protruding from the inner lateral wall of the nasal wall	et I–III (*Manis*)	ft = 2 (*Manis*)	present (*Manis*)	present (*Manis*)	elongated rostrocaudally and dorsoventrally (*Manis*)	Jollie 1968
	carnivorans	branching	protruding from the inner lateral wall of the nasal wall	et I–III (*Canis*, *Felis*, *Meles*, *Mustela, Ursus*) et I–IV (*Halichoerus*) et I–V (*Nasua*)	ft = 3 (*Canis*, *Felis*)	present (*Canis*, *Felis*, *Halichoerus*, *Panthera*)	present (*Canis*, *Felis*, *Panthera*)	reduced	Allen 1882; Fawcett 1892; Paulli 1900a, 1900c; Negus 1958; Hillenius 1994; Van Valkenburgh et al. 2004, 2011, 2014b; Wagner and Ruf 2020

The characteristics of the shape of the maxilloturbinal is determined with reference to Negus 1958.

Conclusion

We constructed 3D models and compared the development of the nasal capsule of five species of prenatal talpids and soricids using the diceCT imaging method. After observing various stages of the development of the nasal capsule, we have identified homologies in turbinal between groups of eulipotyphlans. Moreover, by mapping the turbinal structure on the recent phylogeny, we proposed a scenario for the turbinal evolution of eulipotyphlans.

As for the ethmoturbinal recess, the interturbinal of talpids protrudes from the inner lateral nasal wall between the ethmoturbinal I pars posterior and the ethmoturbinal II, and the epiturbinal protrudes from the ethmoturbinal II. Similar structures are observed in erinaceids and other laurasiatherians according to previous studies. The identification of turbinals was inconsistent for soricids between studies. We here identified the "accessory" of the ethmoturbinal I of soricines as the interturbinal based on our Dice CT imagings of soricids and histological sections of *Sorex* by Parker (1885) and de Beer (1929). Furthermore, soricids do not have an epiturbinal dorsal to ethmoturbinal II, which suggests that the epiturbinal was absent in the common ancestor of soricids.

The maxilloturbinal of erinaceids and solenodontids shows multiple branching. In contrast, the maxilloturbinal of talpids and soricids have only two to three lamellae. Therefore, based on the maximum parsimony, we can assume that the small maxilloturbinal is the result of convergent evolution, which occurred independently in talpids and soricids.

Nevertheless, given that the development pattern of the maxilloturbinal is consistent in eulipotyphlans, we can deduce another scenario. The maxilloturbinal in the common ancestor of eulipotyphlans had few lamellae and was small. Then the maxilloturbinal of the common ancestor of erinaceids, solenodontids, and soricids increased the number of lamellae and size. The number of lamellae and size reduced again in soricids. To discuss which scenario is more credible, we must observe the progressive development of the maxilloturbinal of both soricids and talpids from fetus to adult. In particular, it is necessary to emphasise the observation of neonates, the period when the structure change of the maxilloturbinal occurs.

In order to resolve the homologies of the turbinal structure, we must: 1) examine the continuous structure of the nasal capsule and the cavity using CT imaging or serial sections and 2) observe various developmental stages from the fetus, neonate to adult. The number of studies is insufficient in some taxa, such as uropsilines (talpids) and solenodontids. To fully understand the turbinal development of eulipotyphlans, we must observe and describe the turbinals and laminae of the fetus, neonate, and adult of various species.

Acknowledgements

KI and DK are extremely honored and pleased to contribute to this special issue celebrating the 80th birthday of Professor Wolfgang Maier. His philosophical and deep thoughts into anatomical evolution and development have greatly influenced our research agendas and shaped our lifelong goals. It has been an irreplaceable fortune to be one of the disciples of Marcelo Sánchez-Villagra, also one of the students of Professor Maier, and to be one of Maier's academic family. We would like to assure that his scientific influence and tradition will continue to thrive and flourish also in the Far East. We are grateful to Shin-ichiro Kawada for allowing us to study his specimens. We thank Ingmar Werneburg and Irina Ruf for planning and editing this wonderful issue. This study was supported by JSPS #22J40028 to KI.

References

Allen H (1882) On a revision of the ethmoid bone in the Mammalia, with special reference to the description of this bone and of the sense of smelling in the Cheiroptera. Bulletin of the Museum of Comparative Zoology 10: 135–171.

Ärnbäck Christle-Linde A (1907) Der Bau der Soricide und ihre Beziehungen zu anderen Säugetieren. Gegenbaurs Morphologisches Jahrbuch 36: 464–514. https://www.biodiversitylibrary.org/item/137795

Barrionuevo FJ, Zurita F, Burgos M, Jiménez R (2004) Developmental stages and growth rate of the mole *Talpa occidentals* (Insectivora, Mammalia). Journal of Mammalogy 85: 120–125. https://doi.org/10.1644/BPR-010

Barrios AW, Quinteiro PS, Salazar I (2014) The nasal cavity of the sheep and its olfactory sensory epithelium. Microscopy Research and Technique 77: 1052–1059. https://doi.org/10.1002/jemt.22436

Burgin CJ, Colella JP, Kahn PL, Upham NS (2018) How many species of mammals are there? Journal of Mammalogy 99: 1–14. https://doi.org/10.1093/jmammal/gyx147

Cretekos CJ, Weatherbee SD, Chen CH, Badwaik NK, Niswander L, Behringer RR, Rasweiler IV JJ (2005) Embryonic staging system for the short-tailed fruit bat, *Carollia perspicillata*, a model organism for the mammalian order Chiroptera, based upon timed pregnancies in captive-bred animals. Developmental Dynamics 233: 721–738. https://doi.org/10.1002/dvdy.20400

de Beer GR (1929) The development of the skull of the shrew. Philosophical Transactions of the Royal Society of London B 217: 411–480.

de Beer GR (1937) The Development of the Vertebrate Skull. Clarendon Press, Oxford, 554 pp.

Dieulafe L (1906) Morphology and embryology of the nasal fossae of vertebrates. Annals of Otology, Rhinology & Laryngology 15: 1–584. https://doi.org/10.1177/000348940601500101

Fawcett E (1892) The primordial cranium of *Poecilophoca weddelli* (Weddell's seal), at the 27 mm. CR length. Journal of Anatomy 52: 412.

Fawcett E (1918) The primordial cranium of *Erinaceus europaeus*. Journal of Anatomy 52: 211.

Frick H (1954) Die Entwicklung und Morphologie des Chondrocraniums von *Myotis* Kaup. Georg Thieme Verlag, Stuttgart, 102 pp.

Ganeshina LV, Vorontsov NN, Chabovsky VI (1957) Comparative morphological study of the nasal cavity structure in certain representatives of the order Insectivora. Zoologicheskii Zhurnal 36: 122–138.

Giannini NP, Macrini TE, Wible JR, Rowe TB, Simmons NB (2012) The internal nasal skeleton of the bat *Pteropus lylei* K. Andersen, 1908 (Chiroptera: Pteropodidae). Annals of Carnegie Museum 81: 1–17.

Gignac PM, Kley NJ (2014) Iodine-enhanced micro-CT imaging: methodological refinements for the study of the soft-tissue anatomy of post-embryonic vertebrates. Journal of Experimental Zoology Part B: Molecular and Developmental Evolution 322: 166–176. https://doi.org/10.1002/jez.b.22561

Gignac PM, Kley NJ, Clarke JA, Colbert MW, Morhardt AC, Cerio D, Cost IN, Cox, PG, Daza JD, Early CM, Echols MS, Henkelman RM, Herdina AN, Holliday CM, Li Z, Mahlow K, Merchant S, Müller J, Orsbon CP, Paluh DJ, Thies ML, Tsai HP, Witmer LM (2016) Diffusible iodine-based contrast-enhanced computed tomography (diceCT): an emerging tool for rapid, high-resolution, 3-D imaging ofmetazoan soft tissues. Journal of Anatomy 228: 889–909. https://doi.org/10.1111/joa.12449

Göbbel L (2000) The external nasal cartilages in Chiroptera: Significance for intraordinal relationships. Journal of Mammalian Evolution 7: 167–201. https://doi.org/10.1023/A:1009436419637

Gunnell GF, Bown TM, Hutchison JH, Bloch JI (2008) Lipotyphla. In: Janis CM, Gunnell GF, Uhen MD (Eds) Evolution of Tertiary Mammals of North America: Volume 2: Small Mammals, Xenarthrans, and Marine Mammals. Cambridge University Press, Cambridge, 89–126. https://doi.org/10.1017/CBO9780511541438.008

Gurtovoi NN (1966) Ecological-morphological differences in the structure of the nasal cavity in the representatives of the orders Insectivora, Chiroptera, and Rodentia. Zoologicheskii Zhurnal 45: 1536–1551.

Hillenius WJ (1992) The evolution of nasal turbinates and mammalian endothermy. Paleobiology 18: 17–29.

Hillenius WJ (1994) Turbinates in therapsids: evidence for Late Permian origins of mammalian endothermy. Evolution 48: 207–229. https://doi.org/10.1038/161162d0

Ioana AN (1970) Etude comparative des comets nasaux chez: *Talpa europaea* L., et *Neomys fodiens* Schreb. (Ord. Insectivora) de Roumanie. Travaux du Museum d'Histoire Naturelle "Grigore Antipa" 10: 359–363.

Ito K, Tu VT, Eiting TP, Nojiri T, Koyabu D (2021) On the embryonic development of the nasal turbinals and their homology in bats. Frontiers in Cell and Developmental Biology 9: 1–19. https://doi.org/10.3389/fcell.2021.613545

Jollie M (1968) The head skeleton of a new-born *Manis javanica* with comments on the ontogeny and phylogeny of the mammal head skeleton. Acta Zoologica 49: 227–305. https://doi.org/10.1111/j.1463-6395.1968.tb00155.x

Kaucka M, Petersen J, Tesarova M, Szarowska B, Kastriti ME, Xie M, Kicheva A, Annusver K, Kasper M, Symmons O, Pan L, Spitz F, Kaiser J, Hovorakova M, Zikmund T, Sunadome K, Matise MP, Wang H, Marklund U, Abdo, H, Ernfors P, Maire P, Wurmser M, Chagin AS, Fried K, Adameyko, I (2018) Signals from the brain and olfactory epithelium control shaping of the mammalian nasal capsule cartilage. eLife 7: 1–27. https://doi.org/10.7554/eLife.34465

Kupke A, Wenisch S, Failing K, Herden C (2016) Intranasal location and immunohistochemical characterization of the equine olfactory epithelium. Frontiers in Neuroanatomy 10. https://doi.org/10.3389/fnana.2016.00097

Kuramoto K (1980) Morphological studies on the nasal turbinates of the musk shrew. Nihon Juigaku Zasshi 42: 377–380.

Larochelle R, Baron G (1989) Comparative morphology and morphometry of the nasal fossae of four species of North American shrews (Soricinae). American Journal of Anatomy 186: 306–314.

Le Gros Clark WE (1951) The projection of the olfactory epithelium on the olfactory bulb in the rabbit. Journal of Neurology, Neurosurgery, and Psychiatry 14: 1–10.

Lozanoff S, Diewert VM (1989) Developmental morphology of the solum nasi in the mouse lemur (*Microcebus murinus*). Journal of Morphology 202: 409–424. https://doi.org/10.1002/jmor.1052020308

Lundeen IK, Kirk EC (2019) Internal nasal morphology of the Eocene primate *Rooneyia viejaensis* and extant Euarchonta: Using μCT scan data to understand and infer patterns of nasal fossa evolution in primates. Journal of Human Evolution 132: 137–73. https://doi.org/10.1016/j.jhevol.2019.04.009

MacDonald D (2009) The Encyclopedia of Mammals. Oxford University Press, Oxford, 936 pp.

Macrini TE (2012) Comparative morphology of the internal nasal skeleton of adult marsupials based on X-ray computed tomography. Bulletin of the American Museum of Natural History 365: 1–91. https://doi.org/10.1206/365.1

Maier W (1980) Nasal structures in Old and New World primates. In Ciochon RL, Chiarelli, AB (Eds) Evolutionary Biology of the New World Monkeys and Continental Drift. Springer, Boston, 219–241. https://doi.org/10.1007/978-1-4684-3764-5_11

Maier W (1983) Morphology of the interorbital region of saimiri sciureus. Folia Primatologica 41: 277–303. https://doi.org/10.1159/000156137

Maier W (1993a) Cranial morphology of the therian common ancestor, as suggested by the adaptations of neonate marsupials. In: Szalay F, Novacek M, McKenna M (Eds) Mammal Phylogeny. Springer, New York, 165–181.

Maier W (1993b) Zur evolutiven und funktionellen Morphologie des Gesichtsschädels der Primaten. Zeitschrift für Morphologie und Anthropologie 79: 279–299.

Maier W (2000) Ontogeny of the nasal capsule in cercopithecoids: a contribution to the comparative and evolutionary morphology of catarrhines. In: Whitehead P, Jolly C (Eds) Old World Monkeys. Cambridge University Press, Cambridge, 99–132. https://doi.org/10.1017/cbo9780511542589.006

Maier W (2002) Zur funktionellen Morphologie der rostralen Nasenknorpel bei Soriciden. Mammalian Biology 67: 1–17. https://doi.org/10.1078/1616-5047-00001

Maier W (2020) A neglected part of the mammalian skull: The outer nasal cartilages as progressive remnants of the chondrocranium. Vertebrate Zoology 2019–2020: 367–382. https://doi.org/10.26049/VZ70-3-2020-09

Maier W, Ruf I (2014) Morphology of the nasal capsule of Primates – with special reference to *Daubentonia* and *Homo*. Anatomical Record 297: 1985–2006. https://doi.org/10.1002/ar.23023

Martineau-Doizé B, Caya I, Martineau GP (1992) Osteogenesis and growth of the nasal ventral conchae of the piglet. Journal of Comparative Pathology 106: 323–331.

Martinez Q, Clavel J, Esselstyn JA, Achmadi AS, Grohé C, Pirot N, Fabre PH (2020) Convergent evolution of olfactory and thermoregulatory capacities in small amphibious mammals. Proceedings of the National Academy of Sciences of the United States of America 117: 8958–8965. https://doi.org/10.1073/pnas.1917836117

Martinez Q, Lebrun R, Achmadi AS, Esselstyn JA, Evans AR, Heaney LR, Miguez RP, Rowe KC, Fabre PH (2018) Convergent evolution of an extreme dietary specialisation, the olfactory system of worm-eating rodents. Scientific Reports 8: 17806. https://doi.org/10.1038/s41598-018-35827-0

McDowell SB (1958) The greater Antillean insectivores. Bulletin of the American Museum of Natural History 115: 113–214. https://doi.org/10.2307/4069997

Michelsson G (1922) Das Chondrocranium des Igels (*Erinaceus europaeus*). Zeitschrift Für Anatomie Und Entwicklungsgeschichte 65: 509–543. https://doi.org/10.1007/bf02593583

Moore WJ (1981) The Mammalian Skull. Cambridge University Press, Cambridge, 369 pp.

Murphy WJ, Eizirik E, O'Brien SJ, Madsen O, Scally M, Douady CJ, Teeling E, Ryder OA, Stanhope MJ, De Jong WW, Springer MS (2001) Resolution of the early placental mammal radiation using bayesian phylogenetics. Science 294: 2348–2351. https://doi.org/10.1126/science.1067179

Negus V (1958) Comparative anatomy and physiology of the nose and paranasal sinuses. Livingstone, London, 402 pp.

Novacek MJ (1986) The skull of leptictid insectivorans and the higher-level classification of eutherian mammals. Bulletin of the American Museum of Natural History 183: 1–112.

Ohdachi SD, Iwasa MA, Nesterenko VA, Hisashi A, Ryuichi M, Werner H (2004) Molecular phylogenetics of Crocidura shrews (Insectivora) in east and central Asia. Journal of Mammalogy 85: 396–403. https://doi.org/10.1644/1383934

Parker WK (1874) On the structure and development of the skull in the pig (*Sus scrofa*). Philosophical Transactions of the Royal Society of London 164: 289–336.

Parker WK (1885) On the structure and development of the skull in the mammalia. Royal Society of London 176: 1–119.

Paulli S (1900a) Über die Pneumaticität des Schädels bei den Säugetieren. Eine morphologische Studie. I. Über den Bau des Siebbeins. Über die Morphologie des Siebbeins und die Pneumaticität bei den Monotremen und den Marsupialiern. Gegenbaurs Morphologisches Jahrbuch 28: 147–178.

Paulli S (1900b) Über die Pneumaticität des Schädels bei den Säugetieren. Eine morphologische Studie. II. Über die Morphologie des Siebbeins und die der Pneumaticität bei den Ungulaten und den Proboscіden. Gegenbaurs Morphologisches Jahrbuch 28: 179–251.

Paulli S (1900c) Über die Pneumaticität des Schädels bei den Säugetieren. Eine morphologische Studie. III. Über die Morphologie des Siebbeins und die der Pneumaticität bei den Insectivoren, Hyracoideen, Chiropteren, Carnivoren, Pinnipedien, Edentaten, Rodentiern, Prosimiern. Gegenbaurs Morphologisches Jahrbuch 28: 483–564.

Reinbach W (1952a) Zur Entwicklung des Primordialcraniums von *Dasypus novemcinctus* Linné (*Tatusia novemcincta* Lesson) I. Zeitschrift für Morphologie und Anthropologie 44: 375–444.

Reinbach W (1952b) Zur Entwicklung des Primordialcraniums von *Dasypus novemcinctus* Linné (*Tatusia novemcincta* Lesson) II. Zeitschrift für Morphologie und Anthropologie 45: 1–72.

Roca AL, Bar-Gal GK, Eizirik E, Helgen KM, Maria R, Springer MS, O'Brien SJ, Murphy WJ (2004) Mesozoic origin for West Indian insectivores. Nature 429: 649–651. https://doi.org/10.1038/nature02597

Rodrigues RF, Rodrigues MN, Franciolli ALR, Carvalho RC, Rigoglio N, Jacob JCF, Gastal EL, Miglino MA (2014) Embryonic and fetal development of the cardiorespiratory apparatus in horses (*Equus caballus*) from 20 to 115 days of gestation. Journal of Cytology & Histology 5: 240. https://doi.org/10.4172/2157-7099.1000240

Rossie JB (2006) Ontogeny and homology of the paranasal sinuses in Platyrrhini (Mammalia: Primates). Journal of Morphology 267: 1–40. https://doi.org/10.1002/jmor.10263

Roux GH (1947) The cranial development of certain ethiopian "Insectivores" and its bearing on the mutual affinities of the group. Acta Zoologica 28: 165–397. https://doi.org/10.1111/j.1463-6395.1947.tb00025.x

Rowe TB, Eiting TP, Macrini TE, Ketcham RA (2005) Organization of the olfactory and respiratory skeleton in the nose of the gray short-tailed opossum *Monodelphis domestica*. Journal of Mammalian Evolution 12: 303–336. https://doi.org/10.1007/s10914-005-5731-5

Ruf I (2004) Vergleichend-ontogenetische Untersuchungen an der Ethmoidalregion der Muroidea (Rodentia, Mammalia). Ein Beitrag zur Morphologie und Systematik der Nagetiere. PhD thesis, Universität Tübingen.

Ruf I (2014) Comparative anatomy and systematic implications of the turbinal skeleton in Lagomorpha (Mammalia). Anatomical Record 297: 2031–2046. https://doi.org/10.1002/ar.23027

Ruf I (2020) Ontogenetic transformations of the ethmoidal region in muroidea (Rodentia, Mammalia): New insights from perinatal stages. Vertebrate Zoology 70: 383–415. https://doi.org/10.26049/VZ70-3-2020-10

Ruf I, Janßen S, Zeller U (2015) The ethmoidal region of the skull of *Ptilocercus lowii* (Ptilocercidae, Scandentia, Mammalia) – a contribution to the reconstruction of the cranial morphotype of primates. Primate Biology 2: 89–110.

Ruf I, Meng J, Fostowicz-Frelik Ł. (2021) Anatomy of the Nasal and Auditory Regions of the Fossil Lagomorph *Palaeolagus haydeni*: Systematic and Evolutionary Implications. Frontiers in Ecology and Evolution 9: 1–12. https://doi.org/10.3389/fevo.2021.636110

Ruf I, Maier W, Rodrigues PG, Schultz CL (2014) Nasal Anatomy of the Non-mammaliaform Cynodont *Brasilitherium riograndensis* (Eucynodontia, Therapsida) Reveals New Insight into Mammalian Evolution. Anatomical Record 297: 2018–2030. https://doi.org/10.1002/ar.23022

Sato JJ, Bradford TM, Armstrong KN, Donnellan SC, Echenique-Diaz LM, Begué-Quiala G, Gámez-Díez J, Yamaguchi N, Nguyen ST, Kita M, Ohdachi SD (2019) Post K-Pg diversification of the mammalian order Eulipotyphla as suggested by phylogenomic analyses of ultra-conserved elements. Molecular Phylogenetics and Evolution 141: 106605. https://doi.org/10.1016/j.ympev.2019.106605

Sato JJ, Ohdachi SD, Echenique-Diaz LM, Borroto-Paéz R, Begué-Quiala G, Delgado-Labañino JL, Gámez-Diéz J, Alvarez-Lemus J, Nguyen ST, Yamaguchi N, Kita M (2016) Molecular phylogenetic analysis of nuclear genes suggests a Cenozoic over-water dispersal origin for the Cuban solenodon. Scientific Reports 6: 1–8. https://doi.org/10.1038/srep31173

Schmidt U, Nadolski A (1979) Die Verteilung von olfaktorischem und respiratorischem Epithel in der Nasenhöhle der Hausspitzmaus, *Crocidura russula* (Soricidae). Zeitschrift für Säugetierkunde 44: 18–25.

Sharma DR (1958) Studies on the anatomy of the Indian insectivore, *Suncus murinus*. Journal of Morphology 102: 427–535.

Smith TD, Bonar CJ (2022) The nasal cavity in agoutis (*Dasyprocta* spp.): a micro-computed tomographic and histological study. Vertebrate Zoology 72: 95–113. https://doi.org/10.3897/vz.72.e76047

Smith TD, Rossie JB (2006) Primate olfaction : anatomy and evolution. In: Brewer W, Castle D, Pantelis C (Eds) Olfaction and the brain: window to the mind. Cambridge University Press, Cambridge, 135–166. https://doi.org/10.1017/CBO9780511543623.010

Smith TD, Rossie JB (2008) Nasal fossa of mouse and dwarf lemurs (Primates, Cheirogaleidae). Anatomical Record 291: 895–915. https://doi.org/10.1002/ar.20724

Smith TD, Rossie JB, Bhatnagar KP (2007) Evolution of the nose and nasal skeleton in primates. Evolutionary Anthropology 16: 132–146. https://doi.org/10.1002/evan.20143

Smith TD, Eiting TP, Rossie JB (2011) Distribution of olfactory and nonolfactory surface area in the nasal fossa of *Microcebus murinus*: implications for microcomputed tomography and airflow studies. Anatomical Record 294: 1217–1225. https://doi.org/10.1002/ar.21411

Smith TD, Eiting TP, Bhatnagar KP (2015) Anatomy of the nasal passages in mammals. In: Doty RL (Ed) Handbook of Olfaction and Gustation (Vol. 3). John Wiley & Sons, New Jersey, 37–62. https://doi.org/10.1002/9781118971758.ch2

Smith TD, Curtis A, Bhatnagar KP, Santana SE (2021a) Fissures, folds, and scrolls: The ontogenetic basis for complexity of the nasal cavity in a fruit bat (*Rousettus leschenaultii*). Anatomical Record 304: 883– 900. https://doi.org/10.1002/ar.24488

Smith TD, DeLeon VB, Eiting TP, Corbin HM, Bhatnagar KP, Santana SE (2021b) Venous networks in the upper airways of bats: A histological and diceCT study. Anatomical Record 1–21. https://doi.org/10.1002/ar.24762

Söllner B, Kraft R (1980) Anatomie und Histologie der Nasenhöhle der Europäischen Wasserspitzmaus, *Neomys fodiens* (Pennant 1771), und anderer mitteleuropäischer Soriciden (Insectivora, Mammalia). Spixiana 3: 251–272.

Springer MS, Murphy WJ, Roca AL (2018) Appropriate fossil calibrations and tree constraints uphold the Mesozoic divergence of solenodons from other extant mammals. Molecular Phylogenetics and Evolution 121: 158–165. https://doi.org/10.1016/j.ympev.2018.01.007

Sterba O (1977) Prenatal development of central European insectivores. Folia Zoologica 26: 27–44.

Symonds MRE (2005) Phylogeny and life histories of the "Insectivora": Controversies and consequences. Biological Reviews of the Cambridge Philosophical Society 80: 93–128. https://doi.org/10.1017/S1464793104006566

Upham NS, Esselstyn JA, Jetz W (2019) Inferring the mammal tree: species-level sets of phylogenies for questions in ecology, evolution, and conservation. PLoS biology, 17: e3000494. https://doi.org/10.1371/journal.pbio.3000494

Van Gilse PHG (1927) The development of the sphenoidal sinus in man and its homology in mammals. Journal of Anatomy 61: 153–166.

Van Valkenburgh B, Smith TD, Craven BA (2014a) Tour of a labyrinth: exploring the vertebrate nose. Anatomical Record 297: 1975–1984. https://doi.org/10.1002/ar.23021

Van Valkenburgh B, Theodor J, Friscia A, Pollack A, Rowe T (2004) Respiratory turbinates of canids and felids: A quantitative comparison. Journal of Zoology 264: 281–293. https://doi.org/10.1017/S0952836904005771

Van Valkenburgh B, Curtis A, Samuels JX, Bird D, Fulkerson B, Meachen-Samuels J, Slater GJ (2011) Aquatic adaptations in the nose of carnivorans: Evidence from the turbinates. Journal of Anatomy 218: 298–310. https://doi.org/10.1111/j.1469-7580.2010.01329.x

Van Valkenburgh B, Pang B, Bird D, Curtis A, Yee K, Wysocki C, Craven BA (2014b) Respiratory and olfactory turbinals in feliform and caniform carnivorans: The influence of snout length. Anatomical Record 297: 2065–2079. https://doi.org/10.1002/ar.23026

Vogel P (1972) Vergleichende Untersuchung zum Ontogenesemodus einheimischer Soriciden (*Crocidura russula*, *Sorex araneus* und *Neomys fodiens*). Revue Suisse de Zoologie 79: 1201–1332.

Voit M (1909) Das Primordialcranium des Kaninchens unter Berücksichtigung der Deckknochen. Anatomische Hefte 38: 425–616. https://doi.org/10.1007/BF02214638

Waddell PJ, Okada N, Hasegawa M (1999) Towards resolving the interordinal relationships of placental mammals. Systematic Biology 48: 1–5.

Wagner F, Ruf I (2019) Who nose the borzoi? Turbinal skeleton in a dolichocephalic dog breed (*Canis lupus familiaris*). Mammalian Biology 94: 106–119. https://doi.org/10.1016/j.mambio.2018.06.005

Wagner F, Ruf I (2020) "Forever young"—postnatal growth inhibition of the turbinal skeleton in brachycephalic dog breeds (*Canis lupus familiaris*). Anatomical Record 2020: 1–36. https://doi.org/10.1002/ar.24422

Wagner JA (1855) Die Säugthiere in Abbildungen nach der Natur, mit Beschreibungen. Weiger, Leipzig, 810 pp.

Wible JR (2008) On the cranial osteology of the Hispaniolan solenodon, *Solenodon paradoxus* Brandt, 1833 (Mammalia, Lipotyphla, Solenodontidae). Annals of Carnegie Museum 77: 321–402. https://doi.org/10.2992/0097-4463-77.3.321

Willows-Munro S, Matthee CA (2009) The evolution of the southern African members of the shrew genus *Myosorex*: Understanding the origin and diversification of a morphologically cryptic group. Molecular Phylogenetics and Evolution 51: 394–398. https://doi.org/10.1016/j.ympev.2009.02.012

Witmer LM (1995) Homology of facial structures in extant archosaurs (birds and crocodilians), with special reference to paranasal pneumaticity and nasal conchae. Journal of Morphology 225: 269–327. https://doi.org/10.1002/jmor.1052250304

Witmer LM, Sampson SD, Solounias N (1999) The proboscis of tapirs (Mammalia: Perissodactyla): A case study in novel narial anatomy. Journal of Zoology 249: 249–267. https://doi.org/10.1017/S0952836999009991

Woehrmann-Repenning A, Meinel W (1977) A comparative study on the nasal fossae of *Tupaia glis* and four insectivores. Anatomischer Anzeiger 142: 331–345.

Woodman N (2018) American recent Eulipotyphla: nesophontids, solenodons, moles, and shrews in the New World. Smithsonian Contributions to Zoology 650: 107. https://doi.org/10.5479/si.1943-6696.650

Youssef EH (1971) The chondrocranium of *Hemiechinus auritus aegyptius* and its comparison with *Erinaceus europaeus*. Cells Tissues Organs 78: 224–254.

Zeller U (1987) Morphogenesis of the mammalian skull with special reference to *Tupaia*. In: Kuhn HJ, Zeller U (Eds) Mammalia Depicta. Parey, Hamburg, 17–50.